

Effects of molecular design parameters on plasticizer performance in poly(vinyl chloride): a comprehensive molecular simulation study

Dongyang Li¹, Kushal Panchal^{1,3}, Naveen Kumar Vasudevan¹, Roozbeh Mafi³,
and Li Xi^{*1,2}

¹Department of Chemical Engineering, McMaster University, Hamilton, Ontario
L8S 4L7, Canada

²School of Computational Science and Engineering, McMaster University,
Hamilton, Ontario L8S 4K1, Canada

³Canadian General Tower, Ltd., Cambridge, Ontario N1R 5T6, Canada

August 15, 2021

*corresponding author: xili@mcmaster.ca

Abstract

Using all-atom molecular simulation, a wide range of plasticizers for poly(vinyl chlorid) (PVC), including ortho- and tere-phthalates, trimellitates, citrates, and various aliphatic dicarboxylates, are systematically studied. We focus on the effects of plasticizer molecular structure on its performance, as measured by performance metrics including its thermodynamic compatibility with PVC, effectiveness of reducing the material's Young's modulus, and migration rate in the PVC matrix. The wide variety of plasticizer types covered in the study allows us to investigate the effects of seven molecular design parameters. Experimental findings about the effects of plasticizer molecular design are also compiled from various literature sources and reviewed. Comparison with experiments establishes the reliability of our simulation predictions. The study aims to provide a comprehensive set of guidelines for the selection and design of high-performance plasticizers at the molecular level. Molecular mechanisms for how each design parameter influences plasticizer performance metrics are also discussed. Moreover, we report a nontrivial dependence of plasticizer migration rate on temperature, which reconciles seemingly conflicting experimental reports on the migration tendency of different plasticizers.

1 Introduction

Plasticizers are usually mixed with amorphous polymers to adjust materials properties and improve their processability. Their addition softens the material and reduces its stiffness, while improves its ductility and flowability at the melt state^{1,2}. Efficiency of a plasticizer is typically measured in terms of the extent of property improvement brought by a given plasticizer dosage. Thermodynamic compatibility with the host polymer is also an important factor which determines whether they can be easily blended. In practice, other considerations such as cost and toxicity also affect the choice of plasticizers. Poly(vinyl chloride) (PVC) is a highly polar polymer in which the C-Cl groups induce strong interactions between repeating units. Pure PVC is stiff and brittle, for which plasticizers are commonly used^{3,4}. According to existing data, there are approximately 500 different plasticizers commercially available and 80% of plasticizer production is consumed by PVC². Phthalates are the most widely used group of plasticizers, which occupies more than 80% of the plasticizer market⁵⁻⁷ due to its excellent plasticization compatibility. However, migration of phthalates out of the host PVC, which could cause potential harm to the environment and human health, has raised concerns in recent years, which caused tightening governmental regulations limiting their application in areas such as food, medical devices, and toys.^{2,8-10} Other types of plasticizers, such as adipates¹¹⁻¹³, trimellitates¹³⁻¹⁵, phosphates^{2,16}, epoxides^{16,17}, and citrates^{11,16,18}, are also commercially available. Many are considered as alternatives to phthalates. Development of new green plasticizers is also an area of strong interest^{7,19-21}. However, understanding of the fundamental relationship between the molecular structure of plasticizers and its performance in PVC remains very limited.

Nearly all available plasticizers share some similarities in their structure. It typically has two or more side chains, referred to as "legs" in this paper, each connected to a central group, the "torso", through a carboxylate ester group (see tables 1 and 5 and appendix A for representative examples). The alkane chain in the legs is also called the alcohol chain in many references. Different types of torsos and legs can be combined to form a variety of plasticizers, while legs can also be attached to the torso at different positions. The effects of these molecular design parameters

(MDPs) on plasticizer performance are not comprehensively understood.

Experimental studies often focus on individual MDPs and, for compatibility and migration tendency, indirect measurements are typically reported. Shaw²²⁻²⁴ and Gilbert²⁵ measured the solid-gel transition temperature of plasticized PVC, from which the Flory-Huggins interaction parameter (χ)²⁶ is calculated using a theoretical model from Anagotstopoulos^{22,27,28}. They concluded that phthalates are more compatible with PVC than adipates do and the compatibility decreases with increasing leg length. Grotz²⁹ used a mass uptake experiment to measure the diffusion coefficient (D) of various phthalates and adipates in rubbery PVC³⁰⁻³², and concluded that, in a temperature range of 353–373 K, the diffusion coefficient of both types of plasticizers decreases with leg length. Different thermomechanical properties have been used to compare plasticizer efficiency, such as glass transition temperature (T_g)^{20,33,34}, hardness^{15,16}, and stress at break^{7,20,21}. Maric and coworkers evaluated the efficiency of many types of plasticizers, including phthalates^{7,19}, adipates¹⁹, succinates^{7,19,20}, maleates²¹, and fumarates^{7,21}, and concluded that maleates (torso: -CH=CH-) and succinates (torso: -CH₂-CH₂-) with a leg length of four to six C atoms exhibited the highest plasticization effect among all plasticizers studied.

Plasticizer design requires coordinated consideration of multiple performance metrics. Very often enhancement of one property is achieved at the expense of another and trade-off becomes inevitable. Meanwhile, the large number of MDPs cannot be covered by any single family of plasticizers. There are only a few more comprehensive experimental studies covering multiple MDPs and multiple properties at the same time. Graham¹⁴ compared five types of plasticizers (adipates, linear-leg phthalates, branched-leg phthalates, trimellitates, and phosphates) based on three performance metrics (volatility, permanence, and efficiency). According to the study, adipates provide high plasticization efficiency but low permanence (i.e., migration resistance), phthalates give high permanence but result in films that are less flexible, trimellitates are important because of their low volatility and high resistance to leaching in aqueous media, and phosphates are generally applied due to their flame retardance. Krauskopf^{15,16} studied the effects of more than ten MDPs (leg length, adding a third leg on the benzene ring, changing the torso from a benzene

ring to an alkane chain, etc.) on the plasticizer performance. Compatibility was estimated by the final gelation temperature¹⁵ and PVC solvency^{16,35} (quantitatively measured by the Hansen solubility interaction radius as estimated with the group contribution method), and diffusivity was calculated from a paraffin oil extraction test³⁶ (plasticizer migrating to oil).

Distilling a clear depiction of the relationship between the MDPs and plasticizer performance from experimental studies has been the focus of a number of reviews and book chapters³⁷⁻³⁹. Compatibility with PVC, plasticization effectiveness or efficiency, and migration tendency are the performance metrics most commonly discussed. Many such efforts were limited to certain types of plasticizers and individual MDPs – e.g., Wypych³⁷ mainly focused on the effects of the side-chain length in phthalates. Attempts of including multiple plasticizer chemical families and different MDPs often led to inconsistent findings and conclusions (see, e.g., Nass and Heiberger³⁹), mostly because experiments from different sources generally used different formulations (plasticizer type and composition), measurement techniques, and experimental protocols, making direct comparison on equal basis impossible.

Major theories for plasticization include the lubricity theory⁴⁰, gel theory⁴¹, and free-volume theory⁴². These theories are all phenomenological in nature and also lack molecular details. None of them is designed to provide direct reliable prediction of plasticizer performance based on its chemical structure. Overall, deeper and more comprehensive understanding of the relationship between common MDPs of plasticizers and all their key performance metrics (compatibility, efficiency, and permanence) is needed in order to better guide the continued search and development of green and effective alternative plasticizers.

Molecular modeling and simulation can be a valuable tool for handling the current challenges of plasticizers. The tool has been widely applied in polymer research for over three decades. Simulation of polymer-additive mixtures is, however, disproportionally uncommon. Wagner et al.⁴³ reported a molecular simulation study on the T_g of a triethylcitrate plasticized polymethacrylate. Despite the relatively short chain length (32 repeating units) used, the study captured the general trend of T_g reduction with increasing plasticizer content, although discrep-

ancies in the quantitative T_g magnitudes between simulation and experiments were also obvious. Abou-Rachid et al.⁴⁴ applied molecular simulation to the evaluation of the compatibility between energetic plasticizers, including dioctyl adipate (DOA) and diethylene glycol dinitrate (DEGDN), with hydroxyl-terminated polybutadiene (HTPB) by computing the enthalpy of vaporization. Zhao et al.⁴⁵ used molecular simulation to investigate the miscibility between N-butyl-N-(2-nitroxy-ethyl)nitramine (Bu-NENA) and bis(2,2-dinitropropyl)formal/acetal (BDNPF/A) with glycidyl azide polymer (GAP) by computing their Flory-Huggins parameters. Both of the above two studies concerned energetic materials for combustion and propulsion applications and used short ($\mathcal{O}(10)$ repeating units) chains in their molecular models. Molecular simulation of plasticizer effects on PVC did not appear until very recently. Using a short-chain (20 repeating units) model PVC system, Zhou and Milner⁴⁶ studied the T_g reduction effect of plasticization by investigating local T_g shifts as an indicator of local chain dynamics around plasticizer molecules.

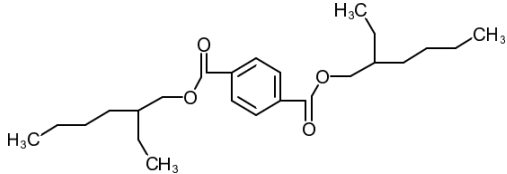
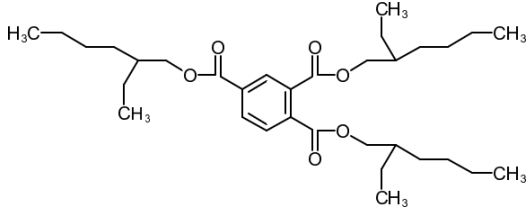
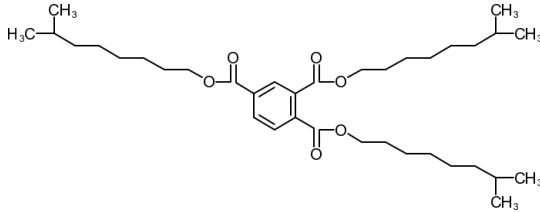
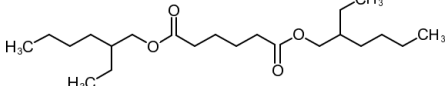
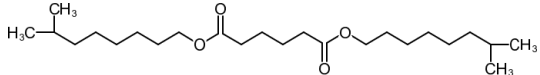
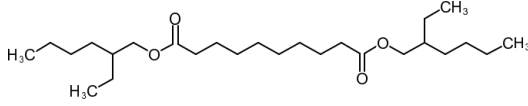
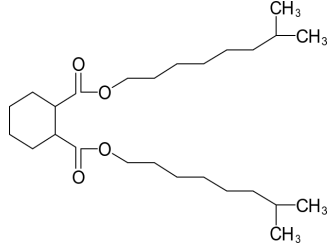
Our ultimate goal is to predict the performance of any given plasticizer from its chemical structure (molecular design). Key performance metrics such as plasticization efficiency and plasticizer permanence require the measurement of dynamical or mechanical properties (e.g., diffusion and stress-strain behaviors) where effects of polymer molecular weight are substantial. In our recent work⁴⁷, a simulation protocol for generating molecular models of plasticized PVC with more realistic chain length ($\mathcal{O}(10^2)$ repeating units) was proposed and validated. The same study also predicted the performance of different plasticizers in the ortho-phthalate family. Comparison between those plasticizers allowed detailed discussion about the effects of one particular MDP – the leg (side chain) length/size. The results were somewhat intuitive: increasing the leg length, which increases both the overall molecular size (thus lowers plasticizer mobility) and the portion of non-polar alkyl chains within the molecule (thus weakens its overall binding with PVC), leads to plasticizers that are both less effective and less compatible with PVC.

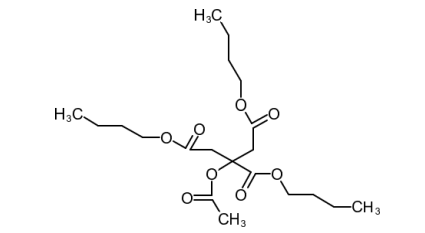
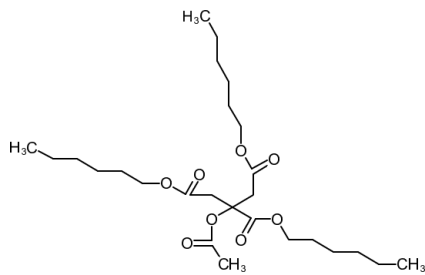
Building on that earlier progress, the current study aims to establish a general set of guidelines for plasticizer design by comprehensively studying all major MDPs. Fourteen commonly used plasticizers are simulated and they are chosen to cover a number of chemical families: ortho-

phthalates with different leg size and branching configurations (DEHP, DIBP, DIOP, DINP, and DITP), terephthalates (DOTP), trimellitates (TOTM and TINTM), different types of aliphatic dicarboxylates (DEHA, DEHS, DINA, and Hexamoll[®] DINCH), and citrates (CA-4 and CA-6). Chemical structures of these compounds are summarized in table 1.

Table 1: Chemical structures of plasticizer molecules modeled in this study (N_C : Number of C atoms in each leg or alkyl side chain).

Common Name	Full name	N_C	Category	Chemical Structure
DEHP	Bis(2-ethylhexyl) phthalate	8	ortho-phthalate	
DIBP	Diisobutyl Phthalate	4	ortho-phthalate	
DIOP	Diisooctyl phthalate	8	ortho-phthalate	
DINP	Diisononyl phthalate	9	ortho-phthalate	
DITP	Diisotridecyl phthalate	13	ortho-phthalate	

DOTP	Diethyl terephthalate	8	terephthalate	
TOTM	Tris(2-ethylhexyl) trimellitate	8	trimellitate	
TINTM	Triisononyl trimellitate	9	trimellitate	
DEHA	Bis(2-ethylhexyl) adipate	8	aliphatic dicarboxylate (adipate)	
DINA	Diisononyl adipate	9	aliphatic dicarboxylate (adipate)	
DEHS	Bis(2-ethylhexyl) sebacate	8	aliphatic dicarboxylate (sebacate)	
Hexamoll® DINCH (Hexamoll or Hexa.)	Diisononyl cyclohexane- 1,2- dicarboxylate	9	aliphatic (alicyclic) dicarboxylate	

Citroflex [®] A-4 (CA-4)	Acetyl tributyl citrate	4	citrate	
Citroflex [®] A-6 (CA-6)	Acetyl trihexyl citrate	6	citrate	

Among them, only the ortho-phthalates were studied in Li et al.⁴⁷, which are still included here not only for completeness, but also for two other reasons: (1) ortho-phthalates provide the benchmark cases with which other plasticizers are compared for studying MDP effects; (2) this study also attempts to further elucidate the molecular mechanisms behind the chemical structure to performance relationship, which was not thoroughly studied in Li et al.⁴⁷.

DOTP was developed by the industry as a replacement for ortho-phthalates, such as DEHP, to circumvent the regulatory pressure of the latter. Hexamoll is an alternative to phthalates developed and marketed by BASF. (We model the cyclohexane ring in Hexamoll in its chair conformation, which is generally thought to be most stable^{7,48}.) Citrates are a group of biocompatible environmentally-friendly alternative plasticizers. All plasticizers studied here are commercially available. They are selected also to represent the wide spectrum of common plasticizers on the market.

We wrap the variations between these chemical structures into seven molecular design parameters (MDPs). (Relationship between plasticizers and MDPs investigated in this study is summarized in fig. 1.

(I) Leg size: measured by the number of C atoms in the alkyl side chain (including both the main and side branches). For example, the leg size increases monotonically in the order of DIBP, DIOP, DINP and DITP. Leg size is also the only varying parameter between CA-4

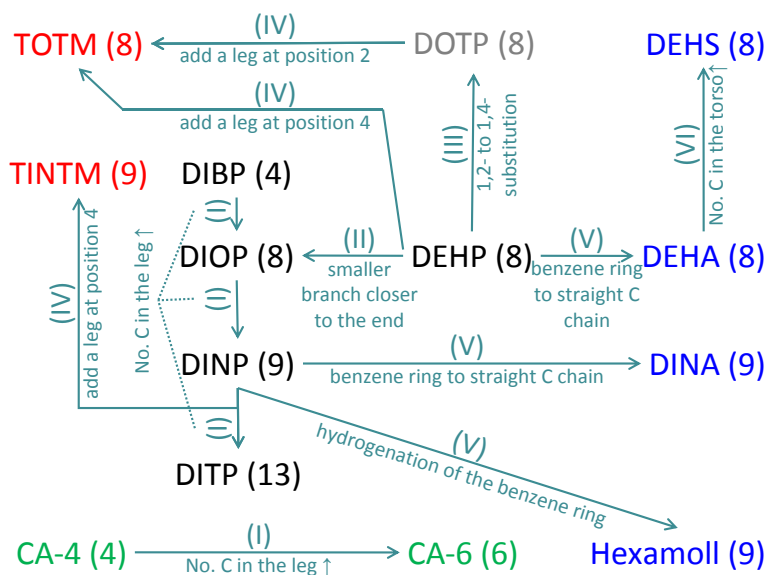


Figure 1: Plasticizers investigated in this study (black for ortho-phthalates, gray for terephthalates, red for trimellitates, blue for aliphatic dicarboxylates, and green for citrates). Roman numerals indicate the molecular design parameter (MDP) varied between each pair. Arabic numerals indicate the total number of C atoms in each leg of the plasticizer (including both main and side branches).

and CA-6.

- (II) Leg branching configuration:** branching position and size of the side chain on the legs. Comparing DEHP and DIOP, both have eight C atoms in each leg, but DEHP has a larger side chain positioned closer to the carboxylate ester group. Similar distinctions are found between TOTM and TINTM and between DEHA and DINA (C numbers in the leg are not strictly equal in these pairs).
- (III) Substitution positions:** ortho- (1,2 substitution – e.g., DEHP) vs. para- (1,4 substitution – i.e., DOTP) substitutions of the legs on the benzene ring;
- (IV) Number of legs:** three legs (1,2,4 substitution) vs. two legs (1,2 or 1,4 substitution) on the benzene ring. TOTM vs. DEHP or DOTP and TINTM vs. DINP are direct comparisons with this parameter varied.
- (V) Torso structure:** replacing the benzene ring with non-aromatic groups. The new torso

group can be acyclic (DEHP vs. DEHA and DEHS) or cyclic (DINP vs. Hexamoll).

(VI) Torso size: between DEHA and DEHS, the only difference is the length of the carbon chain in the torso group.

(VII) Citrate structure: citrates (CA-4 and CA-6) have a distinct quaternary C atom in the torso connecting 3 legs (through carboxylate ester groups) plus 1 acetate group. It is thus listed separately from the rest.

Effects of these MDPs will be discussed by comparing the performance metrics of the corresponding groups or pairs of plasticizers, including the heat of mixing ΔH for plasticizer compatibility with PVC, Young’s modulus of plasticized PVC for its efficiency, and plasticizer mean square displacement (MSD) for its migration tendency. In this paper, we will first give an overview of key observations and discuss the effects of each MDP on these property metrics. It will be followed by further discussion on the molecular origin of those effects. We will then conclude with general guidelines for plasticizer design.

Discussion of phenomenological observations from our simulation will be integrated with a critical synthesis of relevant previous experimental studies to give a comprehensive picture of how each MDP affects each performance metric or indicator. Since previous experiments did not necessarily investigate the same group of plasticizers as this study, chemical structures of plasticizers referenced in our discussion but not covered in our simulation are provided in appendix A and table 5 for the convenience of the reader.

2 Simulation details

All-atom molecular models are used with the polymer consistent force field (PCFF)^{49,50}. Conformations of PVC chains and plasticizer molecules are first generated using the open-source software `Xenoview`⁵¹. PVC conformations are generated by sampling backbone torsion angles following the rotational isomeric state (RIS) model, under the geometric constraint of no atom overlaps, and packed in a periodic cubic cell with a low initial density ($< 0.5 \text{ g/cm}^3$), leaving

ample space for the insertion of plasticizer molecules using Packmol⁵². From this initial configuration, a multistep model equilibration protocol using molecular dynamics (MD) is used to prepare the PVC-plasticizer mixture cell for production run. The initial configuration from XENOVIEW and Packmol first undergoes an energy minimization step, which is followed by a 5 ns NVT simulation at 600K during which only plasticizers are allowed to relax and polymer conformations are kept frozen. After another short (2 ns) NVT run with simultaneous relaxation of both components, the cell density is gradually ramped up to 0.8 g/cm³ and a 2–3 ns NPT (1 atm and 600 K) run follows for the density to converge. A total of 5-7 heating-cooling (300–600 K) cycles (each with 5 ns heating and 8 ns cooling periods) are then applied for the full equilibration of molecular conformations. For every system reported in this study, three random initial configurations are generated with XENOVIEW and Packmol, purposefully at three different initial densities – 0.35 g/cm³, 0.40 g/cm³ and 0.45 g/cm³. After the above equilibration protocol, the size of simulation box converges to the same magnitude regardless of the initial density. Uncertainties reported below are all standard errors between such independent configurations. For details of the equilibration protocol, including its validation, the reader is referred to Li et al.⁴⁷.

Each plasticized PVC cell contains approximately 79wt% PVC (5 atactic chains, each with 300 repeating units) and 21wt% plasticizer. The converged cell dimension at 300 K and 1 atm is 53.77–54.43 Å (with variation between different plasticizers) in each side. Specific composition and final density of each cell are summarized in table 2. All MD simulations are performed with the Large-scale Atomic/Molecular Massively Parallel Simulator (LAMMPS) package⁵³. A cutoff of 15 Å is applied for pairwise – van der Waals (vdW) and electrostatic – interactions. Tail correction is applied to compensate the truncation of long-range vdW interaction^{54,55}, while long-range electrostatic interaction is approximated by the Ewald summation approach^{55–57}. Energy minimization is performed with the conjugate gradient algorithm^{55,56}. The standard velocity-Verlet algorithm with a time step of 1 fs is applied for time integration in MD. Nosé-Hoover chains⁵⁸ are used for thermo- and baro-stats.

Simulation cells of pure PVC (5 chains) and pure plasticizers are also prepared and their com-

Table 2: Compositions and densities of the final equilibrated PVC-Plasticizer mixture cells.

	Number of plasticizer molecules	Number of PVC chains	Repeating units per chain	Plasticizer weight fraction	Final density at 300 K and 1 atm (g/cm ³)
DEHP+PVC	64	5	300	0.210	1.237 ± 0.002
DIBP+PVC	90	5	300	0.211	1.265 ± 0.001
DIOP+PVC	64	5	300	0.210	1.237 ± 0.001
DINP+PVC	60	5	300	0.211	1.233 ± 0.002
DITP+PVC	47	5	300	0.210	1.220 ± 0.001
DOTP+PVC	64	5	300	0.210	1.238 ± 0.001
TOTM+PVC	46	5	300	0.211	1.237 ± 0.001
TINTM+PVC	42	5	300	0.210	1.236 ± 0.002
DEHA+PVC	67	5	300	0.211	1.219 ± 0.001
DINA+PVC	63	5	300	0.211	1.215 ± 0.002
DEHS+PVC	59	5	300	0.212	1.212 ± 0.001
Hexa.+PVC	60	5	300	0.211	1.221 ± 0.002
CA-4+PVC	62	5	300	0.210	1.269 ± 0.001
CA-6+PVC	51	5	300	0.210	1.250 ± 0.001

Table 3: Comparison of the density and solubility parameter of pure plasticizers and pure PVC from our MD simulation with reference values from the literature. MD results for DEHP, DIBP, DIOP, and DITP were previously reported in Li et al.⁴⁷. Reference density values were from experiments. Reference values for the solubility parameter were estimated with the group contribution method by Small⁵⁹.

Pure	Density (g/cm ³)		Solubility Parameter ((J/cm ³) ^{1/2})	
	MD (26.85°C)	Expt. (20°C)	MD (26.85°C)	Ref. (25°C)
DEHP	0.948 ± 0.001	0.984 ⁶⁰	19.46 ± 0.12	18.18 ⁶¹
DIBP	1.030 ± 0.001	1.039 ⁶⁰	20.23 ± 0.04	18.76 ⁶²
DIOP	0.950 ± 0.003	0.983 ⁶⁰	18.87 ± 0.04	18.10 ⁶²
DINP	0.937 ± 0.001	0.975 ⁶⁰	18.52 ± 0.05	18.04 ⁶²
DITP	0.898 ± 0.001	0.952 ⁶⁰	18.48 ± 0.05	17.41 ⁶¹
DOTP	0.951 ± 0.001	0.983 ⁶³	18.74 ± 0.01	-
TOTM	0.955 ± 0.001	0.991 ⁶⁰	18.03 ± 0.05	18.53 ⁶¹
TINTM	0.941 ± 0.001	0.977 ⁶⁴	19.08 ± 0.05	-
DEHA	0.895 ± 0.001	0.929 ⁶⁰ (25°C)	17.83 ± 0.01	17.42 ⁶¹
DINA	0.887 ± 0.001	0.929 ⁶⁰	18.61 ± 0.01	-
DEHS	0.881 ± 0.001	0.912 ⁶⁵ (25°C)	17.46 ± 0.01	17.36 ⁶¹
Hexamoll	0.906 ± 0.001	-	16.46 ± 0.02	-
CA-4	1.047 ± 0.001	1.047 ⁶⁶ (25°C)	20.35 ± 0.01	-
CA-6	0.989 ± 0.001	1.005 ³⁷	19.55 ± 0.02	-
PVC	1.36 ± 0.001	1.35 ~ 1.45 ⁶⁷	16.50 ± 0.02	19.35 ⁶⁸

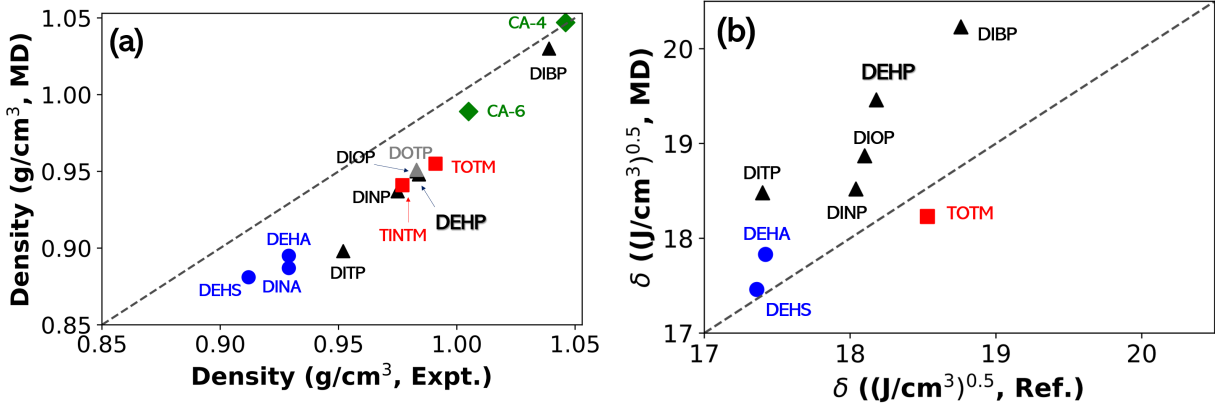


Figure 2: Comparison between the computed density (a) and solubility parameter (b) and reference values (experiments at a lower temperature of 20 °C for density and group contribution method for solubility parameter). All plotted data come from table 3. The dashed diagonal line shows the limit of perfect agreement.

puted properties, including density and solubility parameter, are listed in table 3. Each pure plasticizer cell contains the same number of molecules as the number of plasticizer molecules in the corresponding mixture (table 2). We have tested larger cells with 100–150 plasticizer molecules and the results are nearly identical. The Hildebrand solubility parameter δ is defined as the square root of cohesive energy density (CED). Specific cohesive energy, E_{coh} , is defined as the difference between, E_{bulk} (the specific potential energy of molecules in the condensed phase), and E_{sep} (the specific potential energy of the same molecules when they are separated infinitely apart). CED is simply a measure of cohesive energy on the basis of unit volume

$$\delta^2 \equiv \text{CED} \equiv \frac{E_{\text{coh}}}{V} \equiv \frac{E_{\text{sep}} - E_{\text{bulk}}}{V} \quad (1)$$

where V is the specific volume. For calculating E_{sep} of pure plasticizer systems, molecules are picked from the cell, one at a time, and moved to an empty cell with its conformation kept frozen^{47,69}. Potential energy of the isolated molecule is recorded and average of 20 randomly picked molecules are used in the calculation. For pure PVC, all five chains are selected one by one to make the same calculation.

Experimental measurements (for density) or empirical model predictions (for solubility pa-

parameter), whenever available, are also listed in table 3. (For DOTP, only Hansen solubility parameters were found³⁵, which is thus not included in table 3.) Comparison with our simulation results is easier to see in fig. 2. Densities calculated from MD are all slightly lower than corresponding experimental values with a shift of around $0.03 \sim 0.04 \text{ g/cm}^3$. This is at least partially accounted for by the temperature difference between MD (300 K) and most experiments (20°C). Except that, our MD results accurately capture the trend of variation between different plasticizers. For solubility parameter, MD prediction is slightly higher than reference values estimated by the group contribution method of Small⁵⁹ for nearly all plasticizers except TOTM. Note that the group contribution method is semi-empirical and contains errors in itself. The general trend of variation with changing plasticizers is still largely consistent between these two approaches.

3 Results and discussion

Properties of plasticized PVC are calculated, compared and discussed in this section. Results and discussion are divided into two parts. Section 3.1 focuses on the phenomenological findings regarding the effects of MDPs on plasticizer performance. Performance metrics including each plasticizer's thermodynamic compatibility with PVC (measured by the heat of mixing ΔH), plasticization efficiency (measured by the reduction in the Young's modulus ΔY compared with pure PVC), and migration tendency (measured by the MSD curves of the plasticizer in the PVC matrix) are reported and compared between plasticizers with varying MDPs. Experimental observations of the performance of various plasticizers are also reviewed from the literature. Performance of different plasticizers, obtained from both our MD simulation and previous experiments, is compared to analyze the effects of each MDP. Section 3.2 offers discussion and further analysis for the molecular understanding of the observations. Obviously, fully revealing the molecular mechanisms behind every observation, especially in complex polymer mixture systems, in a single study would be impossible. Our discussion will nonetheless shed light on the molecular origins of the MDP effects, which provides the basis for future fundamental investigation.

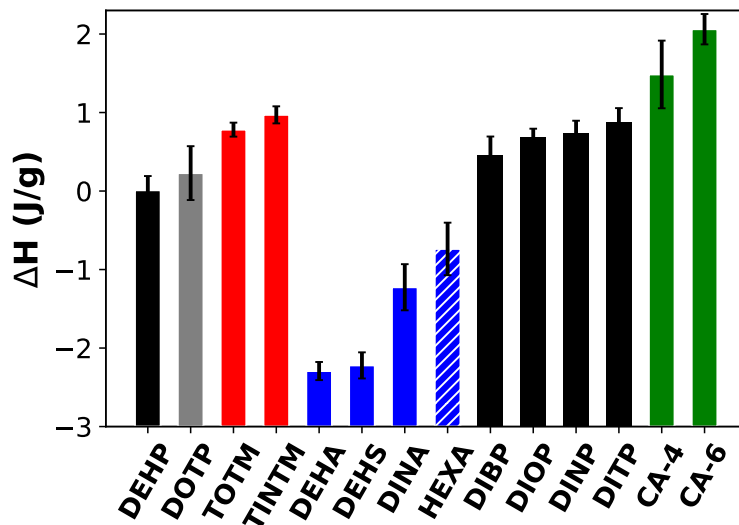


Figure 3: Heat of mixing between PVC and different plasticizers (300 K and 1 atm). Different families of plasticizers are indicated by colors: black for ortho-phthalates, gray for terephthalates, red for trimellitates, blue for aliphatic dicarboxylates (plain for acyclic and slanted for cyclic torso groups), and green for citrates.

3.1 Phenomenological observations

3.1.1 Thermodynamic compatibility

Thermodynamic compatibility or miscibility between the components determines how adequately the constituents can blend into a well-dispersed mixture. Recent attention to plasticizer migration has drawn further attention to this attribute, as plasticizers with higher affinity with the host polymer also have lower thermodynamic tendency to migrate. This is of course only the thermodynamic factor. Diffusion rate is also an important measure for migration, which we will discuss in section 3.1.3.

One empirical method to estimate the miscibility is by comparing the solubility parameter: species with similar δ are commonly presumed to mix well. However, this rule only applies to non-polar species with no specific interactions⁷⁰, whereas the interaction between plasticizer and PVC is clearly nontrivial. Indeed, our earlier work showed that even for ortho-phthalates, this rule does not render any viable prediction and, for polymers, the solubility parameter itself is not a uniquely defined quantity which instead varies with chain length⁴⁷.

The thermodynamic quantity more closely related with miscibility, which is also rather straightforward to calculate in molecular simulation, is the specific heat of mixing

$$\Delta H \equiv H_{p+a} - w_p H_p - w_a H_a \quad (2)$$

where H_{p+a} , H_p and H_a are the specific enthalpy of the mixture, pure polymer, and pure additive (plasticizer), respectively, and w_p and w_a are the corresponding mass fractions. ΔH between each of all fourteen plasticizers under investigation with PVC is plotted in fig. 3. *Higher* ΔH indicates less favorable interactions between components and thus *lower* compatibility. One may point out that the exact quantity for describing the thermodynamic compatibility between components is the Gibbs free energy change of mixing ΔG . By focusing on ΔH as the main indicator, we are making the expedient assumption of neglecting the entropy contribution which is obviously very difficult to compute in polymer systems. Considering that all plasticizers are comparable in size and chemical nature in comparison with PVC, it is not too far-fetched to assume that the entropy change ΔS of mixing different plasticizers with PVC at the same mass fraction does not vary much. For a smaller group of ortho-phthalates, we have previously showed that prediction of compatibility based on ΔH is consistent with experimental observations⁴⁷. Viability of this approach will be further examined here for a much larger and more diverse pool of plasticizers.

Review of Experimental Methods Before we proceed to discuss the specific effects of each MDP, we will first review the common experimental methods for studying plasticizer compatibility with PVC. These methods were seen in previous experiments that we will reference. Knowing the specific experimental techniques provides the essential context to properly interpret the results. The reader is reminded that for plasticizers not listed in table 1, they can refer to appendix A and table 5 for the chemical structures.

Plastisol Gelation Temperature A suspension of PVC resin particles in a liquid plasticizer phase, also called a plastisol, turns into a gel at sufficiently high temperature. Lower gelation temperature indicates easier penetration of plasticizer molecules into the PVC matrix

and thus better compatibility. This interpretation is obviously simplified as diffusion also affects the onset of gelation – note that dynamical factors cannot be totally excluded from the measurement which is typically conducted by increasing the sample temperature at a fixed rate. Assuming that diffusion is more important at the beginning of the gelation process, when plasticizers just start to soak into the PVC particles, and its effects diminish at later stages of the transition, Krauskopf¹⁵ proposed to use the final gelation temperature from dynamic mechanic analysis (DMA) as an indicator for compatibility. Van Oosterhout and Gilbert²⁵ used a simpler optical criterion and measured the clear point – defined as the temperature at which the mixture becomes clear during the gelation process. At least for plasticizers commonly tested in both studies, the measured clear point is close to the final gelation temperature by Krauskopf¹⁵ (difference $\sim \mathcal{O}(10)^\circ\text{C}$ or lower). They then used a relationship proposed originally by Flory²⁶ and modified by Anagostopoulos²⁷ to estimate the Flory-Huggins interaction parameter χ from the clear point temperature and compared the results with χ predicted from the UNIFAC-FV model (based on the group contribution method).

Fourier Transform Infrared Spectroscopy (FTIR) The method is based on the assumption that strongly interacting components will have their mixture FTIR spectrum to deviate significantly from the linear superposition of pure-species spectra. For PVC mixtures with various plasticizers, González and Fernández-Berridi¹³ observed changes and shifts in absorption bands corresponding to the stretching vibration of the C–Cl group of PVC and carbonyl group of plasticizers – the most polar groups of both components. (However, as we will show in section 3.2.1, interaction between these groups does not totally account for all observed changes in compatibility between different plasticizers.) They then quantified this effect by focusing on the fraction of the atactic band in the combined tactic-atactic region of C–Cl stretching and the percentage change in this fraction is used as the indicator for compatibility – larger change corresponds to better compatibility.

MDP Effects We now discuss the specific effects of varying each MDP, as defined in section 1, on plasticizer compatibility with PVC according to both our simulation and previous experimental results.

(I) Leg size

Comparing ortho-phthalates of the same family, the compatibility with PVC, according to fig. 3, follows the order of DIBP (4) > DIOP (8) > DINP (9) > DITP (13). (Note: hereinafter, the number of C atoms in the alkyl side chain, including those on the branch if existent, is indicated between the parentheses). These molecules have nearly identical configurations with leg size being the only varying MDP. It is clear that increasing the leg length reduces compatibility. This finding is consistent with the clear point (gelation) temperature measurements of Van Oosterhout and Gilbert²⁵ where the compatibility decreases in the order of DIBP (4) \gtrsim DBP (4) > DINP (9) \gtrsim DIDP (10) > DIUP (11) > DTDP (13). Note that their list contains two different types of leg branching configurations: DBP and DTDP (appendix A) have straight legs whereas DIBP, DINP, DIDP and DIUP have their legs bifurcating near the end. FTIR measurements by González and Fernández-Berridi¹³ also used plasticizers of different leg branching configurations but the overall trend they found (for PVC films containing 30wt% plasticizers), with the compatibility order of DBP (4) > DEHP (8) > DIDP (10), is again consistent with our conclusion. The same trend is shown in citrates as well. Our simulation shows CA-4 to have higher compatibility than CA-6. We are however unable to find corresponding experimental results.

(II) Leg branching configuration

Except citrates, other plasticizers covered in our MD simulation represent two types of leg branching configurations. One is the 2-ethylhexyl group (seen in DEHP, DOTP, TOTM, DEHA, and DEHS) and the other are isoalkyl groups of varying length with a methyl group attached to the penultimate C atom of the main chain (seen in DIBP, DIOP, DINP, DITP, TINTM, DINA, and Hexamoll). Comparing DEHP with DIOP, both containing a total of eight C atoms in each leg, having a longer side branch closer to the ester group (DEHP)

leads to substantially lower ΔH and higher compatibility (than DIOP). One may argue that for a longer side branch, the main branch is shorter, which seems to suggest that effects of this MDP may be absorbed into the previous one if we replace the latter with the main-branch C number. However, this difference in main branch length (six C atoms in DEHP vs. seven in DIOP) is not sufficient to account for the large increase in compatibility, especially noting that the ΔH of DEHP is even lower than DIBP (three C atoms in the main branch). The same observation is made when comparing the compatibility of trimellitates, TOTM (8) > TINTM (9), and of aliphatic dicarboxylates, DEHA (8) > DINA (9), although those pairs do not have identical leg C numbers. González and Fernández-Berridi¹³ found in their FTIR study that DnOP (8) and 911P (9-11), both having linear legs, show lower compatibility than branched counterparts with comparable C numbers – DEHP (8) and DIDP (10). Similar findings were found in the clear point measurements of Van Oosterhout and Gilbert²⁵ (compatibility: DIBP (4) > DBP (4) and DIUP (11) > DUP (11); in both cases, plasticizers with linear legs, DBP and DUP, are less compatible with PVC) and in the final gelation temperatures reported by Krauskopf¹⁵ (DEHA and TOTM are more compatible with PVC than DINA and TINTM, respectively). We may thus conclude that for legs with similar C numbers, increasing degree of branching improves the compatibility with PVC. (For the DEHP vs. DIOP comparison, although both have one branch in each leg, the branch in DEHP is longer and closer to the torso. Thus the effects seem stronger.)

(III) Substitution positions

Comparing DEHP and DOTP, which have identical leg size and configuration, changing the position of substitution from the ortho-position (1,2-substitution) to the para-position (1,4-substitution) slightly reduces the plasticizer compatibility with PVC and the difference is no larger than the statistical uncertainty of our simulation. DOTP still appears to be more compatible with PVC than those with isoalkyl side chains (e.g., DIOP). We are again unable to find experimental results of DOTP in the literature.

(IV) Number of legs

TOTM has three legs substituted at the 1, 2, and 4 positions of the ring. Compared with DEHP and DOTP, both of which have identical ethylhexyl legs as TOTM, adding a third leg significantly decreases the plasticizer's compatibility with PVC. Similar observation can be made between DINP and TINTM (both with isononyl legs), although the increase of ΔH due to the third leg is smaller than the DEHP-TOTM comparison. Overall, TOTM has the highest ΔH (least compatible with PVC) among all phthalates studied. Even compared with DITP, which has more combined leg C atoms (26 from two legs, compared with 24 from three legs in TOTM), ΔH of TOTM is still higher. Experimentally, González and Fernández-Berridi¹³ also found TOTM to be less compatible with PVC than DEHP from their FTIR analysis. Krauskopf¹⁵ found worse compatibility of TOTM and TINTM compared with DEHP and DINP, respectively, by quantitatively comparing their final gelation temperatures ($\approx 15^\circ\text{C}$ higher after adding the third leg). Experiments and MD simulation again converge to the same conclusion on this MDP.

(V) Torso structure

From fig. 3, our MD results indicate that replacing the benzene ring in the plasticizer's torso group by non-aromatic groups significantly improves its compatibility with PVC. Comparing Hexamoll (9) with DINP (9) (both with isononyl legs), hydrogenation of the benzene ring (DINP) into a cyclohexane ring (Hexamoll) substantially reduces ΔH and increases plasticizer compatibility. Relinquishing the ring structure altogether has a stronger effect: comparing DEHA (8) and DEHS (8) with DEHP (8) (all with ethylhexyl legs), ΔH is reduced by over 2 J/g when the benzene ring is replaced with linear carbon chains. Reduction from DINP (9) to DINA (9) is comparable in magnitude. This observation is however opposite to experimental conclusions. Krauskopf¹⁵ reported a small increase ($\sim 5\text{--}10^\circ\text{C}$) in the final gelation temperature (decrease in compatibility) from DEHP to DEHA and from DINP to DINA. Van Oosterhout and Gilbert²⁵ also reported moderate increases in the clear point ($\mathcal{O}(10)^\circ\text{C}$) from DEHP to DEHA and DEHS. FTIR analysis of González and Fernández-

Berridi¹³ also suggested stronger interaction of DEHP with PVC and that of DEHA. The origin of this discrepancy is not clear. Experiments all rely on indirect measurements and are inevitably limited by the specific measurement technique and its underlying assumptions. Meanwhile, in MD simulation thermodynamic quantities are computed directly as defined and also simulation cells can be generated with perfectly uniform distribution of components in the mixture (which is not always guaranteed in experimental blends). Thus, one may expect MD results to be more truthful. On the other hand, MD simulation is at most as accurate as its force field is. Like other classical force fields, PCFF is not polarizable, which may underestimate the interaction between the plasticizer benzene ring with polar groups on PVC and thus underestimate the compatibility of aromatic plasticizers.

(VI) Torso size

From DEHA to DEHS, the number of C atoms on the torso – linear chain between ester groups – increases from 4 to 8 while the legs remain the same. Our reported ΔH of DEHS is only slightly higher than that of DEHA, which would indicate a small decrease of compatibility with increasing torso size. However, the change is much smaller than the statistical uncertainty in the data. Both FTIR¹³ and clear point²⁵ measurements led to the same conclusion: e.g., the clear point temperature increases from 136 °C to 148 °C from DEHA to DEHS²⁵.

(VII) Citrate structure

Citrates are the least compatible (with PVC) group of plasticizers tested. CA-4 has four alkyl C atoms on each leg, which is the same as DIBP (4), but it has a ~ 1 J/g increase in ΔH from that of DIBP. This is similar to the TOTM case in that a three-legged plasticizer has significantly reduced compatibility compared with traditional two-legged ones. Similarly, the ΔH of CA-6 is 1–2 J/g higher than that of DEHP and DIOP. (Ortho-phthalates with 6-C legs, which would be of equal leg length as CA-6, will have lower ΔH than DIOP per the leg-size effects discussed above.) We are again unable to find experimental data on citrates

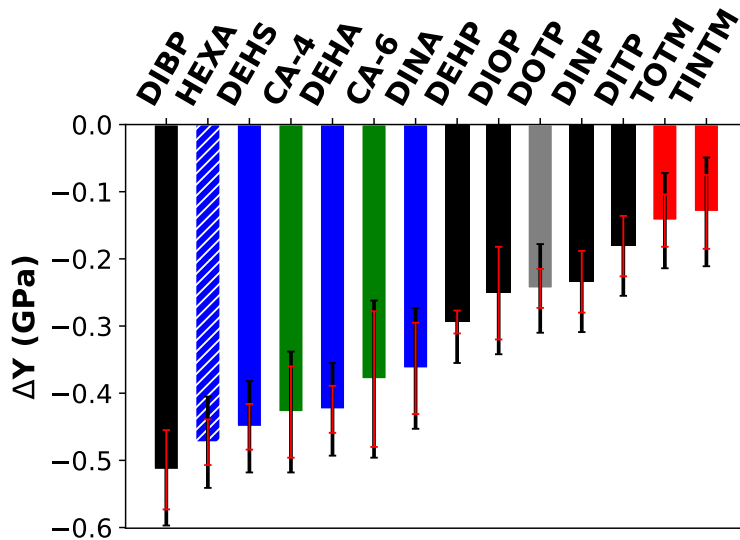


Figure 4: Change of Young’s modulus caused by different plasticizers at 300 K and 1 atm. The Young’s modulus of pure PVC measured in our simulation is $Y = (2.448 \pm 0.059)$ GPa. Bar colors indicate plasticizer type – see fig. 3 caption. Two tiers of error bars are shown for each case: the smaller error bars show the uncertainty of Y of PVC containing each plasticizer and the larger error bars reflect the propagation of uncertainty from the uncertainties in the values of both pure and plasticized PVC.

for comparison.

3.1.2 Plasticization efficiency

Plasticization efficiency can be measured in terms of the reduction in various thermomechanical quantities, such as T_g ^{21,33,71}, hardness^{15,37}, Young’s modulus⁷², apparent modulus^{7,20,21}, torsional modulus^{7,20,21}, etc. It would be unrealistic to investigate all those properties in one single study, many of which, such as T_g , remain costly to calculate. We will thus limit our MD calculation to Young’s modulus. Although, loosely speaking, all mentioned quantities measure the “softening” of materials by plasticizers, they are not all equivalent and there is no guarantee that each plasticizer affects different properties in the same way⁷³. Because of the wide variety of material properties measured in experiments for evaluating plasticization efficiency, in our discussion below we will often have to draw comparison between plasticizer effects on different properties in different studies. This factor should be kept in mind while interpreting any

discrepancy between studies.

In MD, tensile elongation tests are realized by deforming the simulation box along the z direction with a controlled domain length profile

$$L_z(t) = L_{z,0}(1 + \dot{\epsilon}t) \quad (3)$$

and a constant engineering strain rate of $\dot{\epsilon} = 5 \times 10^8 \text{ s}^{-1}$ is controlled, where $L_{z,0}$ is the equilibrium domain length. A pressure of 1 atm is maintained in x and y directions. The tensile stress

$$s = -P_{zz} + \frac{1}{2}(P_{xx} + P_{yy}) \quad (4)$$

(where P_{xx} , P_{yy} , and P_{zz} are the normal x , y , and z components of the negative stress tensor, respectively) and engineering strain

$$e \equiv \frac{L_z - L_{z,0}}{L_{z,0}} \quad (5)$$

are recorded at a 0.1 ps time interval during the tensile deformation. The stress-strain relationship is linear at the limit of small deformation. Young's modulus is calculated by the slope of the stress-strain curve

$$Y \equiv \lim_{e \rightarrow 0} \frac{ds}{de} \quad (6)$$

at the small-strain limit. In this study, the slope is obtained from the linear regression of the stress-strain curve within the $e \leq 0.02$ range.

Compared with our previous study⁴⁷, further effort is made to improve statistical precision by repeating the tensile elongation test 50 times from each system configuration with different randomly assigned initial velocities. This is then repeated for all three independent configura-

tions generated for each case. Uncertainty is calculated treating the 50-trajectory average of each configuration as an independent measurement. For pure PVC, the value reported in this study, $Y = (2.448 \pm 0.059)$ GPa, is within the margin of error of $Y = (2.623 \pm 0.189)$ GPa reported previously in Li et al.⁴⁷ but has much smaller uncertainty.

Figure 4 reports the difference in Y between plasticized and pure PVC

$$\Delta Y \equiv Y_{p+a} - Y_p. \quad (7)$$

The larger error bars in the figure show the propagation of uncertainty

$$\delta(\Delta Y) = \sqrt{\delta Y_{p+a}^2 + \delta Y_p^2} \quad (8)$$

from both Y_{p+a} and Y_p (δ indicates uncertainty). It measures the statistical error in the quantitative value of ΔY . Most of our discussion concerns the efficiency comparison between different plasticizers, to which the smaller error bars (δY_{p+a}) is relevant, because all cases are subtracted by the same Y_p (with the same δY_p).

Since all cases have the same mass fraction of plasticizers, a larger Y reduction reflects higher plasticizer efficiency. Therefore, from left to right in fig. 4, plasticizer efficiency decreases. To compare them by categories, we observe the plasticizer efficiency to decrease in the order: aliphatic dicarboxylates > citrates > ortho-phthalates > terephthalates > trimellitates, although within the same category, e.g., ortho-phthalates, efficiency also varies significantly with changing leg size.

Review of Experimental Methods Before discussing the MDP effects in detail, we will again review major experimental techniques for evaluating plasticizer efficiency.

Tensile Stiffness Tensile tests are widely used in experiments and most closely related with our chosen indicator of Young's modulus. Indeed, the latter reflects the material's tensile stiffness at the small-strain limit. In experiments, the full stress-strain curves are usually measured. The maximum stress (tensile strength) and strain at break are typically reported

and used as the basis for comparing plasticizer efficiency – see, e.g., Ramos-de Valle and Gilbert³³, Erythropel et al.⁷, and Wang et al.³⁴. Erythropel et al.⁷ also reported the apparent modulus (local slope of the stress-strain curve) at 25% strain – Young’s modulus was not measured because of the difficulty of identifying a linear region in experimental stress-strain curves. Comparing the effects of different plasticizers, variation in apparent modulus largely correlates with that in maximum stress – plasticizers giving higher maximum stress usually also give higher apparent modulus. However, maximum stress and strain at break do not show strong correlation.

Dynamic Moduli Storage (G') and loss moduli (G'') can be measured over wide frequency and temperature sweeps in DMA, although it is common to compare their magnitudes at a specified frequency level between PVC samples with different plasticizers. Erythropel et al.⁷ reported G' and G'' magnitudes at 25 °C for different plasticized PVC samples in an oscillatory torsional (twisting) motion. Ramos-de Valle and Gilbert³³ used an eccentric setup (i.e., there is a lateral displacement between the axes of rotation of the two parallel plates) and reported G' and complex viscosity magnitude $(1/\omega)\sqrt{G'^2 + G''^2}$ at a much higher temperature of 140 °C. In both studies, dynamic moduli and maximum tensile stress measurements were reported for the same groups of plasticizers. There appears to be some level of correlation between these metrics – e.g., a plasticizer giving high maximum tensile stress has a higher chance to show high dynamic moduli magnitudes. Exceptions to this correlation are, however, plenty, including some very strong deviations, which is not surprising considering their different modes of motion (shear/twisting vs. extension and oscillation vs. one-way deformation).

Shear Modulus Graham¹⁴ compared the low-temperature shear modulus and room-temperature modulus (the study did not specify the type of modulus used – we assume it was also shear modulus) of PVC with different plasticizers. Plasticizers investigated in the study were referred to by their types (e.g., adipate, linear-legged phthalate, etc.) only without giving

specific chemical names or structures. The low-temperature efficiency largely correlates with the room-temperature modulus with some moderate scattering. For example, linear-legged phthalate shows better lower-temperature efficiency while its performance at room temperature is similar (or slightly worse) compared with branched-legged phthalate.

Glass Transition Temperature T_g Reduction in T_g is perhaps the most examined metric of plasticization effects. T_g can be measured with a variety of techniques. Studies focusing plasticizer performance typically choose mechanical approaches. For example, Ramos-de Valle and Gilbert³³ used thermomechanical analysis and Wang et al.³⁴ used DMA. Phenomenologically, T_g reduction can also be interpreted as “softening” of the material, which resonates with the reduction in stiffness or Young’s modulus. However, there is no guarantee that these two metrics of plasticization must be correlated. Indeed, it is possible for plasticizers with a stronger T_g reduction effect to be ineffective at reducing Young’s modulus⁷³.

Surface Hardness Surface hardness of plasticized PVC samples is measured through indentation tests. Krauskopf¹⁵ used a durometer which measures a material’s resistance to surface indentation and reports the result in a durometer scale. Erythropel et al.⁷ used a micro-indenter which reports surface hardness in terms of the slope of the stress-strain curve during the unloading of the indenter. Compared with maximum stress and apparent modulus reported in the same study, there is some correlation between surface hardness and tensile test measurements, but substantial scattering is also observed (i.e., the same tensile stiffness may map to a wide range of surface hardness). In an extreme case, among different plasticizers tested in that study, PVC plasticized by DEHP showed highest tensile stiffness but lowest surface hardness.

Experimental samples typically contain ~30–40wt% plasticizers (in the same order of magnitude as but higher than our model). Plasticization efficiency is usually assessed by comparing material properties at the same plasticizer weight fraction: i.e., lower stiffness, lower T_g , or lower

hardness indicates more effective plasticizers. Krauskopf¹⁵ quantified the relative efficiency of a plasticizer with its “substitution factor” (SF), defined as the amount of the plasticizer (measured in p.h.r. or parts per hundred rubber) required to achieve a certain material property level (durometer hardness in that study) divided by that of DEHP for the same property level. A SF larger than one indicates the plasticizer to be less effective than DEHP. Graham¹⁴ reported the low-temperature efficiency of a plasticizer in terms of the temperature level at which its PVC sample reach a certain shear modulus level – obviously, lower number indicates a more effective plasticizer at least at low temperatures.

MDP Effects We now look at the effects of each MDP.

(I) Leg size

According to our simulation (fig. 4), among ortho-phthalates, plasticizer efficiency is inversely correlated with the leg size. DIBP (4), which has the shortest legs, is the most effective. DITP (13) has the longest legs and is also the least effective in that group. Similarly, CA-4 is slightly more effective than CA-6. Experimentally, leg size effects on tensile stiffness were reported by Erythropel et al.⁷ for succinates and maleates (appendix A), both types have a straight hydrocarbon chain as the torso group (instead of a benzene ring in phthalates). Both maximum tensile stress and apparent modulus show non-monotonic trends with increasing leg size, with minimums (highest efficiency) found at the leg size of four (DBSu and DBM) or six (DHSu and DHM) C atoms. In our simulation, the shortest legs have four C atoms. As such, we cannot verify whether shorter legs would also give higher Young’s modulus. However, our simulation and Erythropel et al.⁷ at least agree that for legs with more than four C atoms, efficiency deteriorates with increasing leg size. Direct comparison for ortho-phthalates can be found in the surface hardness measurements by Krauskopf¹⁵, which reported the order of efficiency of DBP (4) > DIHepP (7) > DIOP (8) > DINP (9) > DIDP (10) > DTDP (13) – although these plasticizers do not have identical leg branching configurations. According to data reported in Erythropel et al.⁷, the effect

of increasing leg size on plasticizer efficiency is consistent from both surface hardness and tensile properties (tensile strength and apparent modulus at 25% strain). Overall, we conclude that plasticizer efficiency decreases with leg size.

(II) Leg branching configuration

Comparing DEHP (8) with DIOP (8), our simulation shows that having a longer branch closer to the torso (2-ethylhexyl group) results in higher plasticizer efficiency. We may as well compare TOTM (8) with TINTM (9) (efficiency TOTM > TINTM) and compare DEHA (8) with DINA (9) (efficiency DEHA > DINA), but these pairs differ in both leg size and branching configuration and changes in both MDPs – increasing leg size and having a smaller branch closer to the end – are expected to reduce plasticizer efficiency (as observed in fig. 4). Effects of changing leg branching configuration is relatively small compared with the statistical uncertainty in our simulation. In experiments, surface hardness measurements of phthalates by Krauskopf¹⁵ are mostly consistent with our observation, where DEHP (8) and DIOP (8) were found to be equally effective while DIOA (8) is slightly less effective than DEHA (8). For succinates and maleates, comparing the maximum tensile stress and apparent modulus (25% strain) of DEHSu (8) vs. DnOSu (8) and DEHM (8) vs. DnOM (8) pairs, Erythropel et al.⁷ reported small (within or comparable to experiment error) improvement of efficiency as the branched 2-ethylhexyl legs are replaced by linear alkyl chains. Direct comparison with our results is complicated by the fact that we did not simulate phthalates with straight linear legs. Graham¹⁴ reported that linear-legged phthalates are slightly less effective than branched-legged ones according to room-temperature (shear) modulus measurements. Overall, effects of this MDP seem small and the direction of change (lower or higher efficiency) due to increasing branching extent seems to be sensitive to the choice of performance metrics and measurement techniques.

(III) Substitution positions

Comparing DEHP (8) and DOTP (8) in our simulation, changing from ortho- to para-substitution

on the benzene ring only slightly reduces plasticizer efficiency. Surface hardness measurements of Krauskopf¹⁵ also reported slightly lower efficiency of DOTP (8) compared with DEHP (8).

(IV) Number of legs

Comparing TOTM (8) with DEHP (8) or DOTP (8) in fig. 4, adding a third leg substantially reduces plasticizer efficiency. The same conclusion is also reached by comparing DINP (9) with TINTM (9). The effect is clearly stronger than changing substitution position (the previous MDP). For experimental comparison, surface hardness measurements by Krauskopf¹⁵ showed TOTM (with a SF of 1.17) to be substantially less effective than DEHP and DOTP (SF 1.03) and also showed that TINTM (SF 1.27) is less effective than DINP (SF 1.06), both of which are consistent with our simulation. Maximum tensile stress measurements reported by Ramos-de Valle and Gilbert³³ showed about 10% increase from PVC plasticized by DEHP to that by TOTM (i.e., the latter is less effective), which agrees with our results at least semi-quantitatively – note that the difference in ΔY between DEHP and TOTM cases in fig. 4, ~ 0.15 GPa, is also one order of magnitude lower than Y_{p+a} (~ 2.0 – 2.5 GPa). TOTM-plasticized PVC also shows higher T_g than the DEHP case – 7 K higher reported by Ramos-de Valle and Gilbert³³ and 13.8 K higher by Wang et al.³⁴.

(V) Torso structure

Comparing aliphatic dicarboxylates with corresponding ortho-phthalates (DEHA (8) or DEHS (8) vs. DEHP (8) and Hexamoll (9) or DINA (9) vs. DINP (9)) in fig. 4, it is clear that replacing the benzene ring with a non-aromatic torso substantially improves plasticizer efficiency. Between the aliphatic groups, a ring (Hexamoll) seems better than a linear chain (DINA). Unlike the order we saw in thermodynamic compatibility (fig. 3), where a cyclic aliphatic torso (Hexamoll) is between aromatic (DINP) and linear (DINA) cases, for plasticization efficiency, replacing the benzene ring with a cyclic aliphatic group leads to larger improvement than an acyclic one. Experimentally, aliphatic dicarboxylates in-

investigated by Erythropel et al.⁷, including succinates, maleates, and Hexamoll, all lead to substantially lower maximum tensile stress and apparent modulus than DEHP does, which corroborates our simulation prediction. Dynamic moduli and surface hardness measurements, however, showed DEHP to be more effective than or at least comparable to aliphatic dicarboxylates, which highlights the occasional discrepancy between different performance metrics. For tensile stiffness reduction and comparing plasticizers with cyclic and acyclic torso groups, Hexamoll outperforms DESu (2) and DEM (2) but its efficiency is surpassed by other succinates and maleates, the latter of which contradicts our observation. Note that in both experiments and our simulation, difference between Hexamoll and linear aliphatic dicarboxylates is small. In our simulation, in particular, the difference is no larger than statistical uncertainty. Ramos-de Valle and Gilbert³³ also reported lower tensile strength for PVC plasticized by DEHA and DEHS than that by DEHP. Contrary to both our simulation and other experiments^{7,33}, Wang et al.³⁴ reported Hexamoll to be less effective than DEHP, leading to higher T_g and higher tensile strength in the plasticized film. Graham¹⁴ reported substantially lower room-temperature (shear) modulus of PVC plasticized by adipates compared with phthalates (both linear- and branched-legged), which is consistent with the tensile stiffness results from our simulation. Surface hardness measurements by Krauskopf¹⁵ also showed DEHA (SF 0.92) to be more effective than DEHP and DINA (SF 0.98) to be more effective than DINP (SF 1.06). We may conclude that, as far as tensile stiffness is concerned, aliphatic dicarboxylates are generally more effective than phthalates, while the difference between cyclic and linear aliphatic torso groups is much smaller. Effects of this MDP on other metrics of plasticizer efficiency can differ.

(VI) Torso size

Comparing DEHA (8), which has four C atoms in the torso group, and DEHS (8), which has eight, the latter shows marginally larger Young's modulus reduction (better efficiency), which is well within statistical uncertainty. Ramos-de Valle and Gilbert³³ reported DEHS to produce slightly lower (~ 2 K) T_g of the film than DEHA does, but its resulting tensile

strength is slightly ($< 5\%$) higher. Despite the inconsistency between different measurements, overall the effects of this MDP is small and often statistically indistinguishable.

(VII) Citrate structure

Per our simulation, CA-4 (4) is somewhat (within statistical error) less effective in reducing Young's modulus than DIBP (4). Although these two plasticizers have different branching configurations (but the same leg size), part of this reduced efficiency may be attributed to citrates having three legs. However, compared with the difference between DEHP (8) and TOTM (8), the efficiency drop in citrates from phthalates of equivalent leg size is smaller. Krauskopf¹⁶ reported CA-4 to be slightly less effective, in terms of tensile strength reduction, than common phthalates DIHepP (7), DIOP (8), DINP (9), and DEHP (8). Wang et al.³⁴ reported the T_g of PVC plasticized by CA-4 to be slightly lower (1.5 K) than that by DEHP but tensile strength is statistically indistinguishable between the two. Neither experiment showed the considerable improvement in plasticization efficiency of CA-4 in comparison with DEHP as observed in our simulation.

3.1.3 Molecular mobility

Plasticizer migration is determined by both thermodynamic and transport factors. The former decides the ultimate tendency for migration loss: i.e. when exposed to a given surrounding (atmosphere, soil, or solvent), how much plasticizers will have to escape before the mixture reaches a thermodynamic equilibrium. This factor is most directly correlated with ΔH examined in section 3.1.1. The transport factor decides how fast it will approach such an equilibrium. It is important in predicting plasticizer loss at the transient stage before the equilibrium is reached (which can take a long time). Plasticizer transport in a polymer matrix is dominated by molecular diffusion. The diffusivity of plasticizers in polymers is difficult to accurately measure in both experiments and simulations. Direct prediction of diffusion in MD requires the calculation of

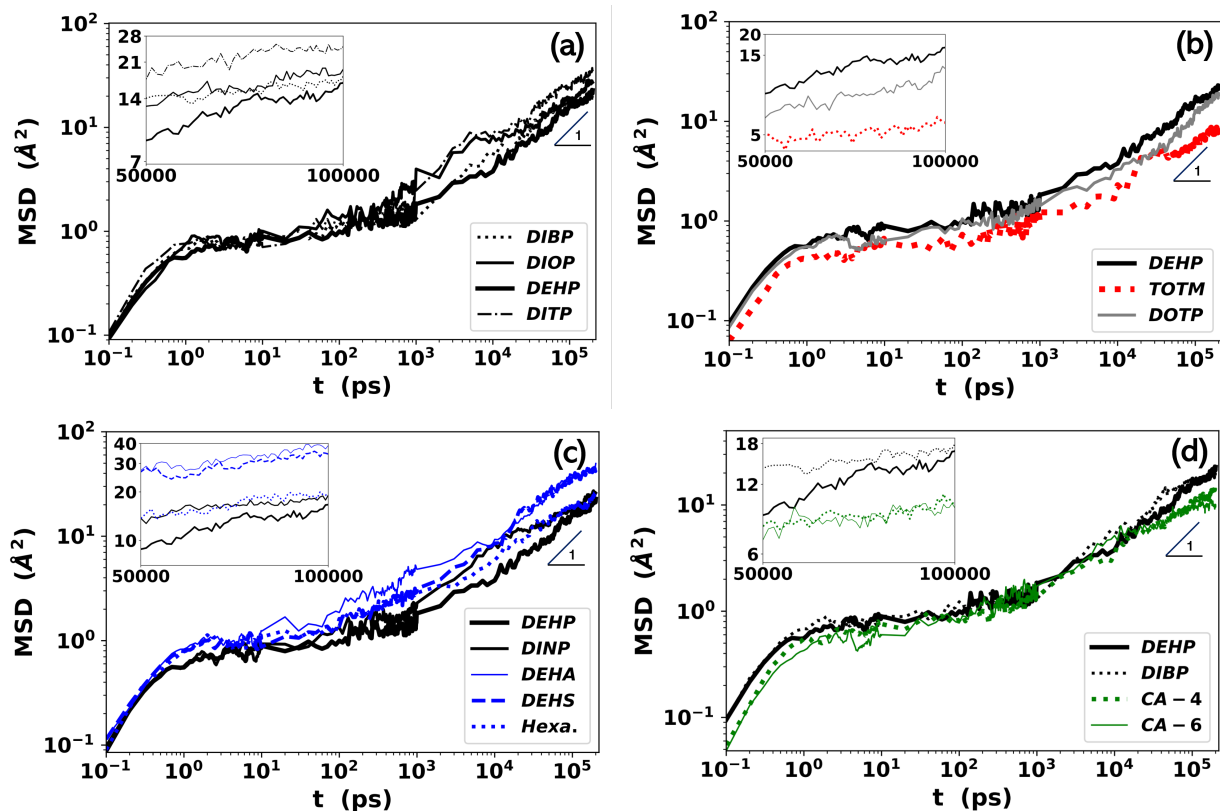


Figure 5: Mean square displacement of the center of mass of all C atoms on the torso of each plasticizer molecule during its diffusion in the PVC matrix (300 K). Comparisons are grouped by MDPs with DEHP used as a common benchmark. Inset in each panel shows the enlarged view of the 50–100 ns range.

mean-square displacement (MSD), which is defined by

$$\langle r^2 \rangle(t) \equiv \langle \vec{r}(t + t_0) - \vec{r}(t_0) \rangle^2 \quad (9)$$

where \vec{r} is the atom position, and $\langle \cdot \rangle$ denotes the average over different time origins t_0 and different particles (atoms/molecules). At the long time limit, $\langle r^2 \rangle$ becomes linear in t according to the Einstein relation

$$\langle r^2 \rangle(t) = 6Dt \quad (10)$$

and diffusivity D can be extracted from the slope of the MSD curve. The challenge is that the time scale required for reaching this limit is beyond the capability of MD simulation.

Figure 5 shows the MSD curves for different plasticizers, using the center of mass (COM) of all C atoms on a plasticizer’s torso group as a marker for tracking its diffusion patterns. Each MSD curve reported here comes from the MD simulation of 200 ns in an NVT ensemble. The time scale covers a wide range of the relaxation spectrum of plasticizers, but for all but a few of them, it does not cover any significant part of the diffusive regime (which would have a slope of 1 in the log-log coordinates of the figure) to extract the diffusivity from eq. (10). We will thus base our discussion on the direct comparison of MSD curves themselves. For the high computational cost of these simulations and the large number of plasticizers to cover, we are not able to have three independent repeats for each case (as we did in ΔH and ΔY). We will thus rely on the intrinsic fluctuations in the MSD curves for estimating the level of uncertainty. To save computational time, we also did not compute MSD curves for TINTM and DINA, given their similarity with TOTM and DEHA.

MSD of DEHP is used as a common reference curve for comparing cases in different panels of fig. 5. The curve starts with a high slope at $t < O(1)$ ps, which captures the fluctuations of the molecule in its local environment. Li et al.⁴⁷ showed that at the same 21% mass fraction, T_g of PVC plasticized by ortho-phthalates measured in MD is in the range of 305 – 310K. At

$T = 300\text{K}$ studied here, which is slightly below T_g , a nearly-flat region appears in the $O(1) - O(10)\text{ps}$ range. This quasi-plateau reflects the “dynamical arrest” or “caging” effect typical of glassy materials: molecules are trapped in a small local “cage” formed by neighboring molecules and polymer segments. The molecule starts to gradually relax from the confining cage at $t = O(100)\text{ps}$ as the MSD curve rises again. Up to the limit of our simulation, i.e., 200ns , the slope is still slightly lower than 1 – i.e., the dynamics still remains in a sub-diffusive regime. Meanwhile, the longest displacement reached by DEHP is about 5 \AA , which is smaller than the size of the whole molecule. Our simulation thus does not fully capture the entire spectrum of molecular relaxation. We may still compare the time scale for different plasticizers to escape the local cage and the MSD magnitude in the sub-diffusive regime. Although it seems plausible to expect the MSD at those scales to correlate with the ultimate diffusion rate, the possibility of a later crossover cannot be ruled out. One example is the DEHA and DEHS comparison in fig. 5(c): although DEHA seems to move faster up to the $O(10)\text{ns}$ time scale, DEHS later catches up. Fluctuations and statistical uncertainty in the MSD further complicate the comparison. For these reasons, we are only able to provide a semi-quantitative discussion on the effects of molecular design parameters on plasticizer mobility. More accurate prediction of diffusion rate is a non-trivial challenge that we defer to future work.

Review of Experimental Methods We will again first review major experimental techniques for evaluating plasticizer diffusion rate or migration tendency.

Radiotracer Method In this method, diffusants in a layer of the material are labeled with a radioactive atom. The radioactively labeled layer is covered by another layer of material containing unlabeled diffusants at the same concentration level. As the radioactive diffusants penetrate the other layer, the apparent activity measured at the initially non-radioactive surface increases with time. A one-dimensional diffusion problem can be solved to relate the temporal profile of surface activity to the diffusion coefficient. The layers are commonly set up with the radioactive layer to total thickness ratio of $\rightarrow 0$ (infinitely small – the “thin-

smear” approach), $1/3$, $1/2$ (the “twin-disk” approach), or $2/3$ ⁷⁴. Park and Hoang⁷⁴, Park and Saleem⁷⁵ and Griffiths et al.^{76, 77} applied the method to study the diffusion coefficients of stabilizers, plasticizers, and other diffusants such as n-hexadecane in PVC. Measurements for plasticizer diffusion were performed in the temperature range of 25–55 °C, which is substantially lower than the T_g of pure PVC ($\approx 80\text{--}90$ °C^{34,38,47}) and closer to the T_g of plasticized PVC ($\approx 20\text{--}35$ °C^{34,47}).

Plasticizer Uptake Grotz²⁹ measured the diffusion coefficient of a given plasticizer by immersing an unplasticized PVC disk in the liquid plasticizer. As the disk is soaked by the plasticizer, its weight increase can be measured over time. Storey et al.³⁰ and Coughlin et al.^{78, 79} pointed out that the boundary condition used by Grotz²⁹ for the diffusion problem was not appropriate for the disk-immersion setup and proposed a corrected solution. For sufficiently small time durations – i.e., before the plasticizer is able to penetrate to the center of the disk, the problem is approximated by two separate processes of diffusion into infinite cylinders. The diffusion coefficient can be obtained by fitting the plasticizer mass uptake over time with the analytical solution. The method earned wide popularity thanks to its accuracy and ease of use^{80,81}.

Solvent Extraction In an opposite process, weight loss of a plasticized PVC sample immersed in an extractant can be used to measure the rate of plasticizer diffusion out of PVC⁸². Introduction of the extractant species further complicates the system, as extractant molecules may enter and dilate the polymer matrix, which would significantly accelerate the diffusion process. High-molecular-weight extractants can be used to minimize this effect. For example, data collected by Cannon and Mahnken, as reported in Nass and Heiberger³⁹, used the ASTM No. 2 oil as the extractant, while Krauskopf¹⁶ used paraffin oil. In principle, the diffusion coefficient can still be obtained through diffusion modeling, although existing literature all tended to report directly the weight loss over a certain fixed time period (e.g., 24 hrs or 96 hrs) directly or its growth rate with increasing time.

Polymer Extraction Marcilla et al.¹¹ monitored plasticizer loss in a PVC film with its surface covered by a polystyrene (PS) film in a controlled-temperature (70 °C, which is only slightly lower than the T_g of pure PVC) environment. Plasticizer concentration change in PVC was tracked from real-time FTIR spectra by measuring the area ratios between characteristic absorption bands of PVC and the plasticizer. The concentration value was obtained through comparison with calibration curves. Diffusion coefficient was again extracted from the temporal profile of plasticizer concentration with the help of diffusion modeling. In an earlier variant of the method, they⁸³ sandwiched a PS film by two plasticized PVC films (at 50 °C) and measured the plasticizer content in PS with thermogravimetric analysis (TGA). Migration tendency was reported in terms of plasticizer uptake by PS over a fixed time period (one week).

Among these approaches, the radiotracer method most closely resembles our simulation setup. Since the two layers have otherwise identical composition expect that in one of them, the diffusing molecules are labeled, this method directly measures the diffusion coefficient in the absence of concentration gradients. All other approaches not only involve substantial spatial variation of plasticizer concentration (concentration gradient), but also temporal variation. Because the diffusion coefficient is very sensitive to plasticizer concentration, diffusion modeling using a constant diffusion coefficient, as commonly used in those approaches, only gives a phenomenologically averaged value over different concentrations. In addition, thermodynamic factors are convoluted with diffusion in mass transfer between phases. For example, thermodynamic compatibility between the extracting phase (solvent or another polymer) and the plasticizer also affects how much plasticizers can be extracted.

Also note that experiments in the literature were performed at a variety of different temperatures, most of which are higher than 300 K used in fig. 5. As we shall discuss in more detail in section 3.2.3, diffusion rate depends non-trivially on temperature. Discrepancy between simulation and experimental temperatures further complicates the comparison.

MDP Effects We now look at the effects of each MDP.

(I) Leg size

In fig. 5(a), MSD curves of ortho-phthalates are statistically indistinguishable within the quasi-plateau region but the order of their escape, as well as their mobility in the sub-diffusive regime, is clearly affected by leg size. Overall, for the same leg type, increasing leg size leads to faster escape. The order of mobility in the sub-diffusive regime is: DITP (13) > DIOP (8) > DIBP (4). Comparison of citrates (fig. 5(e)), however, does not show obvious differences linked to leg size. This could be attributed to the small difference in leg size between CA-4 and CA-6. Our conclusion is consistent with the radiotracer experiments at 308.2 K and 315.8 K by Griffiths et al.⁷⁶, which showed the diffusion coefficient to follow an order of DDP (10) > DHP (6) > DBP (4). Their follow-up study⁷⁷ also showed the same trend at 25 °C, but departure from this trend was observed as temperature increases and such departure seemed more likely at higher plasticizer concentration. Marcilla et al.⁸³, however, reported an opposite trend in their PS-extraction/TGA experiments. For three phthalates with non-identical leg branching configurations, they reported the migration rate to follow the order of DHepP (7) > DEHP (8) > DINP (9). The same trend was also reported between citrates of identical leg branching configuration: CA-2 (2) > CA-4 (4) > CA-6 (6). Similar trends were also reported in their later PS-extraction/FTIR study¹¹ for phthalates, adipates, and citrates. Compared with Griffiths et al.^{76,77}, these authors not only used a different measurement method, migration rate was also measured at much higher temperatures of 50–70 °C. Plasticizer uptake experiments at 80–100 °C by Storey et al.³⁰ also obtained an opposite dependence (to that of Griffiths et al.^{76,77} and ours) on leg size: DPP (5) > DHP (6) > DHepP (7) > DnOP (8) > DNP (9) > DDP (10). Most other migration experiments were performed at similarly raised temperatures and they also reported the decrease of diffusion rate or migration tendency with longer legs^{84,85}. Overall, the increasing diffusion rate with increasing leg size, as predicted by our simulation, is only consistent with the radiotracer measurements^{76,77} at near-room-temperature conditions.

(II) Leg branching configuration

Comparison between DIOP (8) and DEHP (8) in fig. 5(a) shows that an increasing degree of branching in DEHP, defined by its longer side branch positioned closer to the torso, slows down its motion. The rise of the DIOP curve slows down after ~ 5 ns, which raises the possibility of a later crossover between DIOP and DEHP. However, it could also be attributed to statistical uncertainty. Our simulation result is consistent with the solvent extraction experiments of Krauskopf¹⁶ where DIOP was also found to have a higher migration tendency than DEHP at 50 °C. Storey et al.³⁰ also found, in their plasticizer uptake experiments, that in terms of diffusion coefficient $D_{nOP} (8) > DIOP (8)$ (80–100 °C) and $DDP (10) > DIDP (10)$ (90 °C). Since D_{nOP} and DDP both have linear alkyl chains, this is again consistent with our general conclusion that a higher degree of branching leads to lower diffusion coefficient and better migration resistance.

(III) Substitution positions

Comparison of DOTP (8) and DEHP (8) in fig. 5(b) shows a clear decrease of mobility after changing from ortho- (1,2) to para- (1,4) substitution of the legs on the benzene ring. We are not able to find experimental diffusion data for direct comparison, but it is known that DOTP does display a higher (than DEHP) resistance to migration into certain nitrocellulose lacquer finishes³⁸.

(IV) Number of legs

Comparison of TOTM (8) and DEHP (8) in fig. 5(b) shows that adding a third leg significantly reduces plasticizer mobility. Unlike changing leg length or configuration (fig. 5(a)), effects of the additional leg are obvious from the short time limit well below the quasi-plateau regime: i.e., local fluctuation within the cage is also suppressed. We are again not able to find experimental data for this design parameter.

(V) Torso structure

Comparing DEHA (8) and DEHS (8) with DEHP (8) as plotted in fig. 5(c), it is clear that

replacing the benzene ring by a linear carbon chain significantly increases plasticizer mobility. The enhancement starts in the sub-ps regime (i.e., before the quasi-plateau) and the plateau itself is also raised. This observation is consistent with experiments. Krauskopf¹⁶ also reported significantly higher leaching tendency for DEHA compared with DEHP (and adipates in general in comparison with ortho-phthalates) from solvent extraction. In the PS-extraction/FTIR experiments by Marcilla et al.¹¹, adipates showed significantly higher diffusion coefficient than corresponding ortho-phthalates. Comparing at the same mass fraction (40.7%) and temperature (70 °C), the diffusion coefficient of DHA (6) is $\approx 40\%$ higher than DHP (6) and for DEHA (8) vs. DEHP (8) and DINA (9) vs. DINP (9) comparisons, the difference is nearly one order of magnitude.

Compared with the drastic speed-up brought by linear torso groups, effects of replacing the benzene ring in phthalates with an alicyclic group (as in Hexamoll) are much less significant. In fig. 5(c), the MSD of Hexamoll (9) is higher than that of DEHP (8) but lower than the linear dicarboxylates DEHA (8) and DEHS (8). More importantly, when compared with DINP (9), which has the same leg configuration, the mobility of Hexamoll (9) is nearly at the same level, indicating that the enhanced diffusion compared with DEHP is due mostly to changing leg length and branching configuration. Experimental data for Hexamoll, or any other alicyclic dicarboxylates, are not available for comparison.

(VI) Torso Size

In fig. 5(c), the MSD of DEHA (8), which has a 4-C torso, is larger than that of DEHS (8), which has an 8-C torso, at least in the intermediate time range of $\mathcal{O}(10^2)$ to $\mathcal{O}(10^4)$ ps. At longer time, the two curves become indistinguishable. Very few experimental studies have tested multiple aliphatic dicarboxylates (which is necessary to examine this MDP). Krauskopf¹⁶'s solvent extraction tests showed DEHAz (8), which has a 7-C torso, to have higher extraction tendency than DEHA (8). The result does not necessarily contradict our simulation. Since, per our simulation, torso size has little effect on molecular diffusion, the solvent extraction process may be dominated by thermodynamic factors. Indeed, as we

have shown above, increasing torso size does decrease plasticizer compatibility with PVC.

(VII) Citrate structure

MSD of CA-4 (4) and CA-6 (6) appears slightly lower than that of ortho-phthalates as shown in fig. 5(d). In addition to DEHP (8), we also included DIBP (4) as a reference because it has the same leg size as CA-4. Discrepancies between citrates and ortho-phthalates become noticeable at $t \gtrsim 10^4$ ps and citrates seem to stay in the sub-diffusive regime (i.e., the slope stays lower) for longer time. Limited experimental data on citrates often disagree with our simulation. Solvent extraction tests by Krauskopf¹⁶ covered two citrates – although CB-6 (similar to CA-6 but with a butyryl, instead of acetyl, group that replaces the hydroxyl hydrogen in citric acid – see appendix A and table 5) shows improved extraction resistance, CA-4 has higher extraction tendency (both in comparison with DEHP). Diffusion coefficients of citrates (CA-2, CA-4, and CA-6), as obtained from PS-extraction experiments by Marcilla et al.⁸³ and Marcilla et al.¹¹, are higher than those of ortho-phthalates (DHP, DEHP, and DINP) of similar molecular weights.

3.1.4 Summary and guidelines for plasticizer molecular design

We have so far discussed the compatibility between plasticizers and PVC, plasticization efficiency, and plasticizer mobility as key performance metrics and how they are affected by each MDP. Key conclusions from all our simulation observations as well as related experimental measurements are summarized in table 4. Once again, the comparison should be interpreted with the various discrepancies between experiments and simulation, in terms of their methodological approaches and quantities being measured, taken into account. Nevertheless, our simulation agrees with available experimental trends in most cases with few exceptions. Some of the exceptions, such as the leg-size effects on plasticizer mobility, can be explained upon further investigation, which we will discuss in section 3.2.

This knowledge of MDP effects on plasticizer performance can be leveraged for molecular design. Since changing a MDP can have opposite effects on different performance metrics, trade-

Table 4: Summary of the effects of each molecular design parameter (MDP) on plasticizer performance metrics: comparison between our simulation and related experimental measurements.

	MDP		Compatibility		Efficiency		Diffusivity/Mobility	
	Name	Change	MD	Expt.	MD	Expt.	MD	Expt.
(I)	Leg size	↑	↓	↓ ^{13,25}	↓	↑↓ ⁷ ↓ ¹⁵	↑	↑ ^{a76,77} ↓ ^{b11,30,83-85}
(II)	Leg branching configuration	branching ^c ↑	↑	↑ ^{13,15,25}	↑≈	↑≈ ^{14,15} ↓≈ ⁷	↓	↓ ^{16,30}
(III)	Substitution positions	ortho- → para-	↓≈	N/A	↓	↓ ¹⁵	↓	N/A
(IV)	Number of legs	↑	↓	↓ ^{13,15,34}	↓	↓ ^{15,33}	↓	N/A
(V)	Torso structure	aromatic → linear aliphatic	↑	↓ ^{13,15,25}	↑	↑ ^{d7,14,15,33}	↑	↑ ^{11,16}
(V)	Torso structure	aromatic → alicyclic	↑	N/A	↑	↑ ⁷	≈	N/A
(VI)	Torso size	C chain length ↑	↓≈	↓ ^{13,25}	↑≈	↓↑≈ ³³	↓≈	↓ ¹⁶
(VII)	Citrate structure	ortho-phthalates → citrates ^e	↓	N/A	↓≈	↓≈ ^{16,34}	↓	↓↑ ¹⁶ ↑ ^{11,83}

^aClose to room temperature.

^bRaised temperature.

^cLarger side branch located closer to the carboxylate ester group is considered a higher degree of branching.

^dEffects on tensile stiffness only; other metrics may differ.

^eCompared at the same leg size.

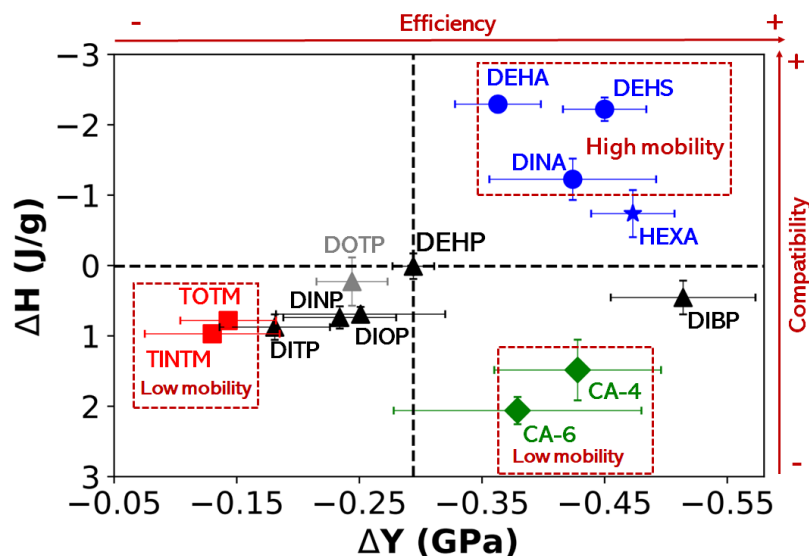


Figure 6: Scatter plots of plasticizer performance in the ΔH - ΔY space. Error bars in ΔY show the uncertainty in the Young's modulus (i.e., the same as the smaller error bars in fig. 4). Text annotations "high mobility" and "low mobility" are in reference to comparison with DEHP.

off is often inevitable to achieve the optimal design for a given application. Figure 6 compares all plasticizers studied in our MD simulation in different performance metrics. Based on DEHP as a common reference for comparison, we make the following observations.

- Ortho-phthalates with isoalkyl legs (lower degree of branching than DEHP) are generally less effective (compared at the same leg size) and less compatible with PVC. They are also subject to higher migration risk.
- Between those ortho-phthalates, decreasing leg size leads to more efficient plasticizers with better compatibility with PVC and also better migration resistance at least at 300 K tested (at higher temperatures the conclusion may differ).
- Adding a third leg substantially improves migration resistance but both efficiency and compatibility will be lower.
- Changing from ortho-phthalates to para-phthalates can improve migration resistance with much smaller reductions in efficiency and compatibility.
- Aliphatic dicarboxylates offer both high efficiency and compatibility, at the expense of migration resistance. Among them, Hexamoll represents a good compromise with substan-

tially improved efficiency and a small increase in migration rate.

- Citrates are more efficient and migration-resistant, but their compatibility with PVC is lower.

3.2 Discussion and molecular interpretation

We now attempt to obtain molecular-level insights behind the above observations. Given the wide scope of parameter space explored in section 3.1 and intrinsic complexity in many of the physical processes, fully understanding the molecular mechanism behind every observation would be an unrealistic target. Here, we try to pick the low-hanging fruit and provide the most obvious answers based on the direct analysis of our simulation results. Inevitably, there will be questions that remain unanswered. We hope that those questions will motivate future research and this study will serve as a gateway to more in-depth investigations into this area.

3.2.1 Thermodynamic compatibility

At the molecular level, PVC segments interact through strong polar-polar interactions between their C-Cl groups. Plasticizers also have polar groups such as the carboxylate ester group, but typically contain a higher portion of non-polar groups such as long alkyl chains. This design can be rationalized through the lubricity theory⁴⁰, which postulates that plasticizers block the polar-polar interactions between polymer segments to facilitate their relative motion. Some polar groups are still needed to maintain a reasonable level of compatibility with the host polymer. As such, to a first approximation, plasticizer compatibility should be proportional to the relative polar content in its structure. As we are comparing different plasticizers at the same mass fraction, for plasticizers with a higher portion of polar groups, more plasticizer-PVC polar-polar interactions are expected, so is better compatibility.

To dissect the contributions to the plasticizer-PVC compatibility, we start by decomposing ΔH in terms of contributions from different types of intermolecular interactions. Note that ΔH is defined as the specific enthalpy change of the isothermal isobaric mixing process. The density

change of this process is small – as we have examined, the $\Delta(PV)$ term is negligible in comparison to energy changes. Also, at the same temperature, the kinetic energy is unchanged. Thus, the enthalpy change of mixing is dominated by the potential energy change of mixing, as indicated by the first \approx relation below

$$\begin{aligned}
\Delta H &\approx \Delta E^{\text{pot}} \equiv E_{\text{p+a}}^{\text{pot}} - w_{\text{p}}E_{\text{p}}^{\text{pot}} - w_{\text{a}}E_{\text{a}}^{\text{pot}} \\
&\sim \Delta E^{\text{inter}} \equiv E_{\text{p+a}}^{\text{inter}} - w_{\text{p}}E_{\text{p}}^{\text{inter}} - w_{\text{a}}E_{\text{a}}^{\text{inter}} \\
&= \Delta E_{\text{vdwl}}^{\text{inter}} + \Delta E_{\text{coul}}^{\text{inter}}
\end{aligned} \tag{11}$$

where “pot” indicates potential energy. We may further assume that the intramolecular part of potential energy does not change substantially upon mixing. Note that this assumption covers both bonded interactions and the intramolecular part of non-bonded interactions. Although it is quite reasonable to assume that the bonded interactions do not change with mixing, the intramolecular non-bonded interactions could still change if mixing causes changes in the molecular conformation. With this assumption, ΔH is dominated by the change of the intermolecular part of potential energy (indicated by “inter”). We use a “ \sim ” sign to indicate this approximation in eq. (11) because, as shown below, it is less accurate. The change in intermolecular interactions of mixing can be further decomposed into terms for the van der Waals (“vdwl”) and Coulombic (“coul”) contributions (the last equality in eq. (11)). Note that our reference to van der Waals interaction includes both the short-range steric repulsion and long-range attraction between atoms – i.e., the full inter-atom interactions captured in the Lennard-Jones potential.

The inter-molecular interactions of mixing between PVC and different plasticizers, ΔE^{inter} , are shown in fig. 7. Should the approximations in eq. (11) be accurate, fig. 7 would be identical to fig. 3. Comparing these two figures, there is clearly a strong similarity between the two quantities. However, quantitative magnitudes do not always match and various levels of discrepancies are found in different plasticizers. These errors mostly come from the neglect of intramolecular non-bonded interactions, indicating that conformation change of molecules does occur during the mixing process. Indeed, the largest discrepancies are found in molecules with highest flexibility

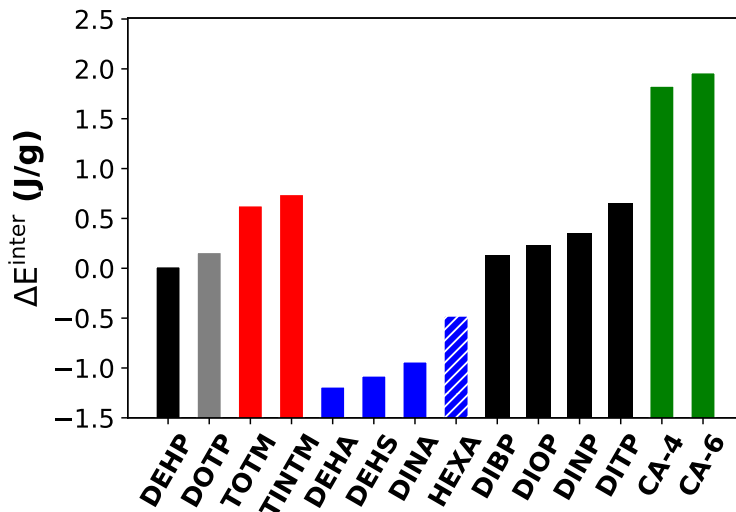


Figure 7: Intermolecular interaction of mixing between PVC and different plasticizers. Bars are colored by plasticizer categories as explained in fig. 3.

– i.e., DEHA and DEHS. Despite the quantitative errors, relative comparison between different plasticizers are completely preserved in ΔE^{inter} . For the purpose of understanding the MDP effects – i.e., why one particular plasticizer has higher ΔH than another, we may neglect the molecular conformation effects and focus on the differences in intermolecular interactions.

Contributions from van der Waals and Coulombic interactions to ΔE^{inter} are shown in fig. 8. Intermolecular interactions are functions of inter-atom distances between molecules which can be quantified using the radial distribution function (RDF) $g(r)$. For its definition, $g_{ij}(r)$ is the number density of type j atoms found at distance r from a reference atom of type i , which is normalized by the domain-average number density of type- j atoms. Figure 9 shows the RDF between the positively charged carbon atom next to the chlorine atom on PVC, $C(-Cl)$, and the negatively charged carbonyl oxygen atom on the plasticizer, $O(=C)$. In all cases, the first peak appears at $\approx 4.5 \text{ \AA}$, which marks the average inter-atom distance between the pair in a typical polar-polar interaction between PVC and the plasticizer. We choose to highlight this RDF based on a simplistic view of plasticizer design, in which the polar carboxylate groups are introduced for the purpose of improving plasticizer compatibility with PVC. In reality, as we will show shortly, polar-polar interaction effects, which would show up in $\Delta E_{\text{coul}}^{\text{inter}}$, can only account for some of the

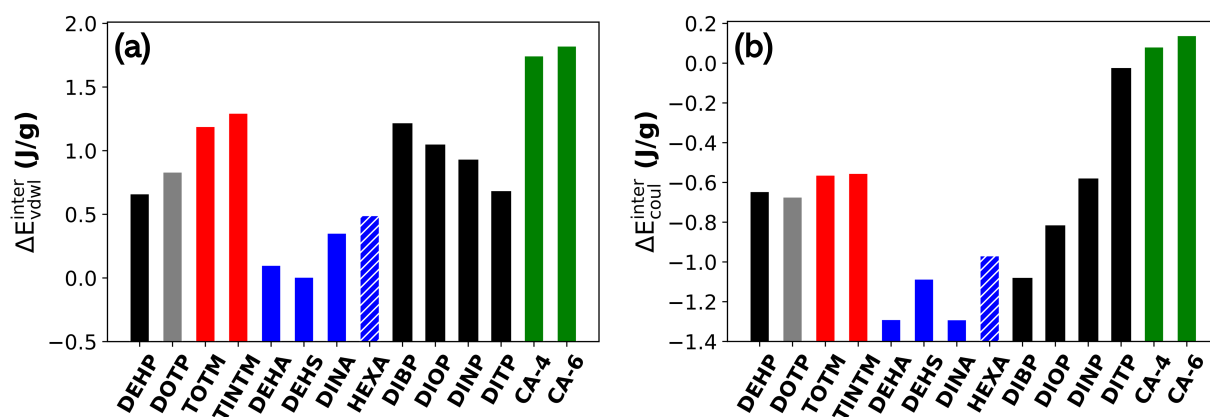


Figure 8: Van der Waals (a) and Coulombic (b) interaction contributions to the intermolecular interaction of mixing shown in fig. 7.

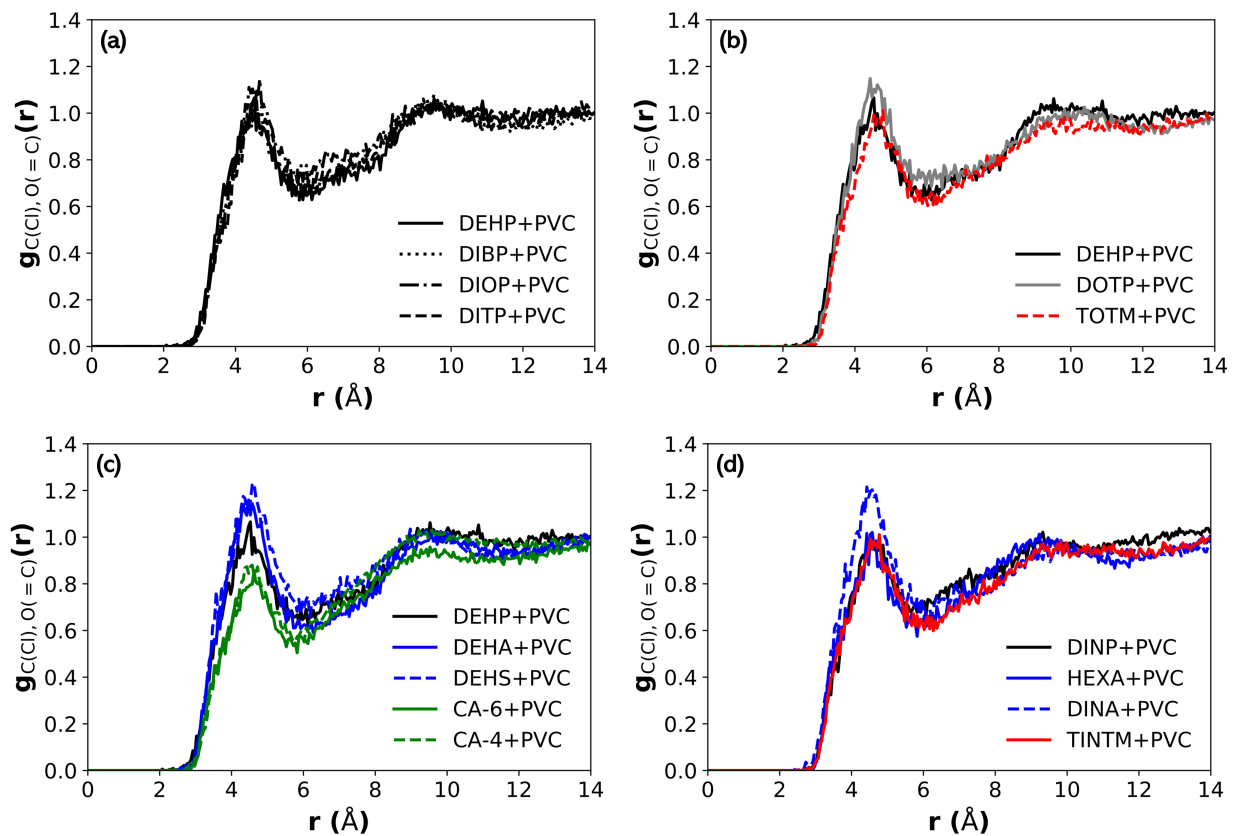


Figure 9: Radial distribution functions (RDFs) between the C atoms bonded with Cl in PVC and the carbonyl O atoms in phthalates $g_{C(-Cl), O(=C)}(r)$ in different PVC-plasticizer mixtures.

observed MDP effects on plasticizer compatibility, whereas $\Delta E_{\text{vdwl}}^{\text{inter}}$ is important for many MDPs.

(I) Leg size

Decreased compatibility with increasing leg length is expected since increasing the length of the alkyl chains increases the proportion of non-polar groups in the molecule. The non-polar alkyl legs can sever polar-polar interactions between C–Cl groups on PVC. Comparing DIBP (4), DIOP (8), DINP(9), and DITP (13) in fig. 8, it is clear that $\Delta E_{\text{vdwl}}^{\text{inter}}$ decreases while $\Delta E_{\text{coul}}^{\text{inter}}$ increases with leg length. The latter effect is much stronger, resulting in the net increase in ΔE^{inter} and thus higher ΔH . Higher $\Delta E_{\text{coul}}^{\text{inter}}$ is consistent with the microscopic picture that favorable polar-polar interactions between PVC segments are increasingly broken up and replaced by less favorable polar (PVC)–non-polar (plasticizer) interactions. Corresponding changes in the RDF, as shown in fig. 9(a), are rather small, indicating that each carbonyl O atom of the plasticizer is nearly equally likely to bind with polar groups on PVC – there are just fewer such polar plasticizer groups in the mixture (at constant mass fraction) as the leg length increases.

(II) Leg branching configuration

According to fig. 8, from DIOP (8) to DEHP (8) increasing the degree of branching substantially reduces $\Delta E_{\text{vdwl}}^{\text{inter}}$ while the change in $\Delta E_{\text{coul}}^{\text{inter}}$ is much smaller. The same pattern is observed in the TINTM (9)/TOTM (8) and DINA (9)/DEHA (8) pairs – both cases involve the same change in branching configuration (although the leg size also differs slightly). These observations clearly indicate that the effects of this MDP are dominated by changes in van der Waals interactions and are tied less to any specific polar-polar interactions (which would have been reflected in $\Delta E_{\text{coul}}^{\text{inter}}$). The specific origin of these changes are much harder to trace and may be partially dynamical – in section 3.2.3, we will show that highly branched legs have lower mobility, which may allow them to stay in energetically more favorable conformations.

(III) Substitution positions

The small increase in ΔH from DEHP (8) to DOTP (8) observed in fig. 3 is attributed to changing van der Waals interactions upon mixing as the Coulombic contribution is nearly the same between the two (fig. 8). Para-substitution has the two legs extending in opposite directions from the aromatic torso group. Compared with ortho-substitution, where contacts between the two legs are more likely, para-substitution minimizes such contacts and allows the legs more exposure to PVC segments. The increased exposure, however, applies to both polar carboxylate groups and non-polar alkyl groups and thus the net effect on $\Delta E_{\text{coul}}^{\text{inter}}$ becomes negligible. The change of exposure itself is also small noting that in fig. 9(b), the RDF peak of DOTP is only marginally higher than that of DEHP. The origin of the small change in $\Delta E_{\text{vdwl}}^{\text{inter}}$ is difficult to identify. On the other hand, the significance of the small change in ΔH is also uncertain given the large uncertainty contained in our DOTP data (fig. 3).

(IV) Number of legs

Comparing the DEHP (8)/TOTM (8) and DINP (9)/TINTM (9) pairs in fig. 8, the significant increase in ΔH (fig. 3) from adding a third leg comes mostly from the increasing $\Delta E_{\text{vdwl}}^{\text{inter}}$ and the difference in $\Delta E_{\text{coul}}^{\text{inter}}$ is much smaller. This pattern is similar to the previous MDP except that the increases in ΔH and $\Delta E_{\text{vdwl}}^{\text{inter}}$ are much larger. Correspondingly, the RDF of TOTM shown in fig. 9(b) is not significantly different from that of DEHP and the same observation is made between DINP and TINTM in fig. 9(d). In both these pairs, the additional leg has the same structure, and thus the same polar content, as the other two. The RDF shows that the polar carbonyl O in three-legged phthalates has the same chance of binding with polar groups on PVC as their two-legged counterparts, which explains the similar $\Delta E_{\text{coul}}^{\text{inter}}$ in corresponding two- and three-legged phthalates. The higher $\Delta E_{\text{vdwl}}^{\text{inter}}$ indicates the presence of unfavorable molecular configuration in the mixture, which is not surprising – it is harder to fit a complex three-legged molecule between polymer segments and thus a plasticizer molecule is more likely to be stuck in a clumsy position.

(V) Torso structure

Comparing DEHP (8) with DEHA (8) and DEHS (8) and comparing DINP (9) with Hexamoll (9), significant reductions are found in both $E_{\text{vdwl}}^{\text{inter}}$ and $E_{\text{coul}}^{\text{inter}}$ (fig. 8) – i.e., van der Waals and Coulombic interaction terms are equally important for the reduction of ΔH and increasing compatibility of aliphatic dicarboxylates. One can rationalize this observation noting that by replacing the aromatic ring in the torso of a plasticizer with an aliphatic group, the overall mobility of the molecule improves. The effect is stronger when the torso group is linear (DEHA and DEHS) than when it is cyclic (Hexamoll). Higher torso flexibility allows both polar carboxylate groups of the same molecule to bind closely with polar groups on PVC, which may not be possible when they are separated by a rigid aromatic ring. Indeed, the RDFs of DEHA and DEHS both display a notably higher peak than that of DEHP in fig. 9(c). Similarly in fig. 9(d), the peak of Hexamoll is much higher than that of DINP. This explains the lower Coulombic part of the potential energy in the mixture. Likewise, we also expect that higher molecular flexibility can allow the molecule to better avoid atom overlaps in the mixture, which would explain the lower $E_{\text{vdwl}}^{\text{inter}}$.

(VI) Torso Size

By the same argument as above, DEHS (8) has a longer torso chain than DEHA (8) and thus has higher torso flexibility. In fig. 8, there is indeed a slight reduction in $\Delta E_{\text{vdwl}}^{\text{inter}}$ from DEHA to DEHS, but $\Delta E_{\text{coul}}^{\text{inter}}$ becomes higher. The RDF in fig. 9(d) does show a higher peak for DEHS, indicating better polar-polar interactions at least between the O(=C) (of the plasticizer) and C(-Cl) (of PVC) atoms. The higher $\Delta E_{\text{coul}}^{\text{inter}}$ can only come from unfavorable interactions from other groups. Similar to the MDP of leg size, increasing torso size (in the case of a non-polar aliphatic torso) also increases the overall non-polar portion in the molecule. This effect can offset that of increasing torso flexibility and the observed change in ΔH (fig. 3) reflects the combined outcome of both effects.

(VII) Citrate structure

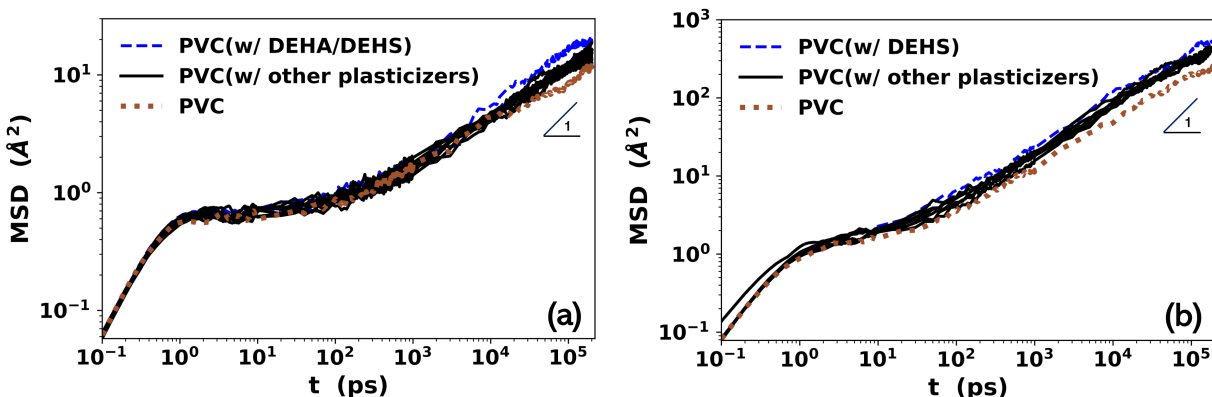


Figure 10: MSD of C atoms on the backbones of plasticized and pure PVC chains: (a) at 300K; (b) at 400K. Cases for PVC plasticized by DEHA or DEHS are colored differently for their notably higher mobility, whereas all other plasticized PVC cases use the same color as their MSD curves are generally indistinguishable.

In fig. 8, citrates show larger contributions from both $\Delta E_{\text{vdwl}}^{\text{inter}}$ and $\Delta E_{\text{coul}}^{\text{inter}}$ than phthates. With three legs and one additional acetate group (in the cases of CA-4 and CA-6), citrates have a total of four polar interaction sites, but they are all connected to one quaternary C atom, which severely restricts the molecule's configurational freedom. As a result, a smaller fraction of them can effectively interact with polar sites on PVC. This is confirmed by the significantly reduced peak magnitude in their RDFs shown in fig. 9(c). Meanwhile, similar to the case of trimellitates, the lack of configurational freedom also increases the chance of unfavorable atom contacts in the mixture, resulting in their higher $\Delta E_{\text{vdwl}}^{\text{inter}}$.

The above discussion clearly shows that the extent of polar-polar interactions between the plasticizer and PVC only partially account for their compatibility. Van der Waals interactions, in particular, the steric repulsion between atoms, are an important consideration in many MDPs. This factor depends on the complex conformation effects of mixing the plasticizer and PVC and is not always straightforward to predict directly from the molecular structure.

3.2.2 Plasticizer efficiency

At the molecular level, the most direct effect of plasticization is accelerated segmental motion of the polymer chains. MSDs of C atoms on PVC backbones are shown for two different tem-

peratures in fig. 10. At the lower temperature (300 K, fig. 10(a)), MSD curves all display a clear quasi-plateau region in the $\mathcal{O}(1)$ ps to $\mathcal{O}(100)$ ps regime and the final stage (200ns) captured is still in the sub-diffusive regime. Within the quasi-plateau, i.e., the “caging” state, dynamics of plasticized PVC chains is not significantly faster than that of pure PVC, which is surprising considering that 300K is only a few degrees lower than the T_g of plasticized PVC (all in the range of 305K to 310K but nearly 50 degrees lower than that of pure PVC (359K) – both quoted T_g values are from molecular simulation reported in Li et al.⁴⁷. In typical glass-forming liquids, a plateau emerges as the temperature approaches T_g and after the glass transition, the plateau grows wider and its height decreases as temperature continues to decrease^{86,87}. The finding that, at such time scales, pure PVC – in its deeply glassy state – has comparable mobility to plasticized PVC, which has just entered the glassy state, indicates that plasticizers do not substantially change the dynamics within the caging stage. This was first reported in Li et al.⁴⁷ for DIOP, but now verified in a much wider range of plasticizers.

Plasticized and pure PVC curves stay close for most of the subdiffusive regime and only separate in the $t > \mathcal{O}(10)$ ns regime. Therefore, we may conclude that plasticizers do not accelerate the local fluctuation when segments are dynamically arrested, but only facilitate the cooperative motions between molecules that help the chain escape from the “cage”. Interestingly, at those longer time scales, PVC mobility plasticized by most plasticizers are similar in magnitude, but linear dicarboxylates (DEHA and DEHS) are particularly effective. At 400K (fig. 10(b)), which is above T_g , the plateau significantly shrinks in size and separation between plasticized and pure PVC occurs at the $\mathcal{O}(10)$ ps regime. Linear dicarboxylates are still the most effective but other plasticizers follow closely behind.

Comparing the MSD results (fig. 10(a)) with those of Young’s modulus (fig. 4), there is some level of similarity: DEHS and DEHA are also among the most effective plasticizers according to the ΔY values, but other highly effective plasticizers, such as DIBP and Hexamoll, do not raise MSD as much. Therefore, changes in macroscopic properties cannot be easily correlated with microscopic chain mobility.

Here, we try to decode the observed MDP effects on mixture Young’s modulus from three perspectives. The first is an energetic perspective. Plasticizers that bind strongly with the host PVC matrix are expected to make the material more resistant to deformation, which gives a higher Young’s modulus. This is essentially the rationale behind the lubricity theory that the introduction of non-polar alkyl leg groups reduces intermolecular binding and thus plasticizes the material. From this perspective, higher compatibility (better binding and lower ΔH) would correlate with lower efficiency (larger resistance to deformation and higher Young’s modulus), which is obviously often not true according to fig. 6. The second is a dynamical perspective. Plasticizers showing higher mobility are easier to find wiggle room as the polymer matrix deforms and thus should give lower Young’s modulus and higher efficiency. In addition to relative movement between molecules, deformation of the material will also induce conformation changes in the constituent molecules themselves. As such, molecules that are more flexible will likely give lower Young’s modulus (higher efficiency). The third is a number argument. Since we are comparing different plasticizers at the same mass fraction, plasticizers with larger molecular weight have lower number density – i.e., within a given volume of the polymer matrix, there are fewer separate “active sites” where plasticizers can take effect, which should contribute to lower efficiency. Admittedly, these rather hand-waving arguments do not constitute a complete theory for explaining plasticization effects, which would require more in-depth investigations in the future. However, we hope these arguments will at least help us rationalize some of the MDP effects on the Young’s modulus of plasticized PVC.

(I) Leg size

According to the lubricity theory⁴⁰, the alkyl chain in the leg acts to block polar-polar interactions between PVC segments. From this energetic perspective, increasing leg length would make such effects stronger. Our observation (fig. 4) is opposite. At the same temperature of 300 K, plasticizer mobility also increases with leg size (fig. 5(a)) whereas PVC chain mobility does not depend strongly on this MDP (fig. 10(a)). Thus the dynamical perspective also cannot explain the lowering efficiency with increasing leg size. We can only resort to

the number density argument, that, for plasticizers of the same type, increasing leg size increases plasticizer molecular weight and thus reduces its number density at the same mass fraction. Based on this argument, if we instead compare at the same number density, the trend would reverse. Indeed, Immergut⁸⁸ and Wurstlin⁸⁹ observed a linear increase in T_g reduction with increasing leg length based on the same plasticizer to PVC molar ratio. The effect of leg size was also discussed in Li et al.⁴⁷ for ortho-phthalates and observations in this study with a wider range of plasticizers are consistent with earlier findings.

(II) Leg branching configuration

As discussed in section 3.1.2, the effects are small and inconclusive. Therefore, we refrain from making any molecular interpretation.

(III) Substitution positions

The effect is relatively small, which again makes a clear mechanistic interpretation difficult. From an energetic or lubricity-theory point of view, para-substitution increases the leg exposure to PVC segments, but the net effect is very small – as we have observed above in fig. 8(b), there is no noticeable difference in $\Delta E_{\text{coul}}^{\text{inter}}$ between DEHP (8) and DOTP (8). These two plasticizers also have the same molecular weight. The only explanation left is molecular mobility. Indeed, according to fig. 5(b), DOTP does show lower mobility than DEHP, which is consistent with its lower efficiency in fig. 4. The cause of this slowdown will be discussed in section 3.2.3.

(IV) Number of legs

TOTM (8) is thermodynamically unfavorable to PVC (fig. 3). From an energetic perspective, weaker binding between TOTM and PVC would predict lower Young's modulus (higher efficiency), which is opposite to our observation. However, TOTM also has significantly lower mobility than DEHP (8) (fig. 5(b)), which from a mobility perspective would give lower efficiency, as observed in fig. 4. In addition, TOTM is also a larger molecule than DEHP or DOTP. Its reduced number density at the same mass fraction also points to the

same direction.

(V) Torso structure

Changing from aromatic to aliphatic (ring or linear) torso group greatly improves efficiency (fig. 4), which is not surprising because aliphatic groups are more flexible with more configurational freedom. For DEHA (8) and DEHS (8), the effect is clearly reflected in not only their own mobility (fig. 5(c)), but also the mobility of PVC chain segments (fig. 10(a)). Notably, their thermodynamic compatibility with PVC is also high – the energetic explanation again fails in this case. Comparing Hexamoll (9) with DINP (9), their mobilities are similar (fig. 5(c)), so are their molecule weights, but Hexamoll is notably more efficient (fig. 4). One may possibly explain this by citing the rigidity of the molecules themselves – flexible torso structures allow the molecule to be deformed with less resistance. However, we are not able to explain why does Hexamoll appear to have comparable efficiency to or even higher efficiency than linear dicarboxylates (fig. 4).

(VI) Torso size

The difference in Young's modulus between DEHA (8) and DEHS (8) is smaller than statistical uncertainty. We again refrain from making any molecular interpretation.

(VII) Citrate structure

Per section 3.1.2, citrates are marginally less efficient than ortho-phthalates when compared at the same leg size (e.g., CA-4 (4) vs. DIBP (4)), but their efficiency is higher than DEHP (8). From the energetic perspective, because of the constraint of the quaternary C atom (as discussed above), their polar carboxylate groups cannot fully access polar groups on PVC, leading to lower thermodynamic affinity and, presumably, lower Young's modulus (higher efficiency). From a mobility point of view, although the mobility of the torso group (quaternary C atom) in citrates is lower than that of DEHP (benzene ring) – see fig. 5(d), MSD of its legs, as shown below in fig. 11(e), is higher for the intermediate time range (quasi-plateau to subdiffusive regimes). DEHP only surpasses both citrates after 50 ns. This means although

citrates may be slower in diffusion, local fluctuation of its legs is stronger, likely also because of the insufficient binding of their carboxylate groups to polar groups on PVC. Since Young's modulus measures the material's resistance to small deformation, local fluctuation is more relevant. This argument predicts lower Young's modulus (higher efficiency). Therefore, although compared with DIBP, which has a smaller molecular weight (278Da), CA-4 (403Da) and CA-6 (487Da) appear to be a bit lower (within uncertainty) in efficiency, they are more efficient than DEHP which has a more comparable molecular weight of 391Da.

Discussion above shows that the energetic argument does not correctly predict the change in Young's modulus in most cases. Instead, dynamical arguments based on molecular mobility and flexibility are more often correct. In the case of a strong disparity in molecular weight, the change in plasticizer number density also becomes important.

3.2.3 Plasticizer mobility

The mechanism of plasticizer molecular diffusion in the PVC matrix is not only central to understanding and predicting plasticizer mobility (migration rate), but also important for explaining their plasticization effects. The latter is clear from our discussion in section 3.2.2, where plasticizer mobility is a key factor in determining their efficiency. Existing knowledge of penetrant diffusion in amorphous polymer matrices is limited to very small guest molecules – gases and simple liquids such as water. Their diffusion follows a so-called “hopping” mechanism where the guest molecules jump between microscopic voids between chain segments in a jerky motion⁹⁰. Plasticizers are much larger in size and more complex in structure. Nearly all of them have backbones consisting of $O(10)$ C atoms arranged into multi-branched configurations with non-trivial specific interactions with the host polymer. Their diffusion has to follow an entirely different process involving non-trivial coupling between conformational changes in both the plasticizer and polymer molecules. Diffusion of longer chain molecules can be described with theories of polymer dynamics⁹¹, which are, however, established mainly for linear chain molecules that are chemically alike to the host matrix⁹². Theoretical description of the diffusion of large and complex

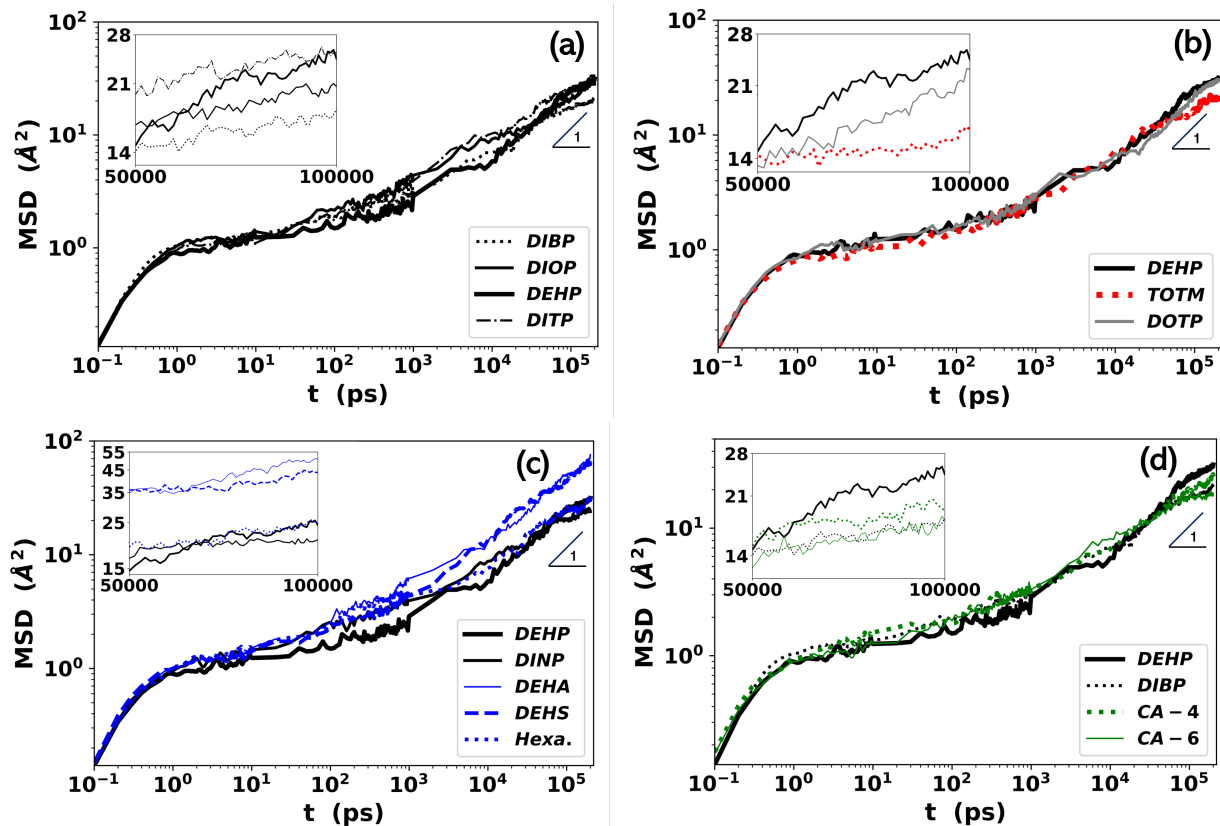


Figure 11: MSD of the center of mass of all C atoms on the legs of plasticizers (300 K). Comparisons are grouped by MDPs with DEHP used as a common benchmark. Inset in each panel shows the enlarged view of the 50–100 ns range.

molecules in polymer matrices is currently not available.

Some insight is still within reach especially considering the similarities between different plasticizers in their chemical structures, which all contain two or more legs connected to a common torso group. In fig. 5, we focused on the MSD of the torso group while here in fig. 11, the MSD of the leg C atoms is displayed. Typically, the legs are longer linear carbon chains with more conformational freedom. For ortho-phthalates, Li et al.⁴⁷ found that their local dynamics, including the quasi-plateau and part of the sub-diffusive regime, is faster than the torso group. The overall plasticizer dynamics is, however, determined by the dynamics of all legs as well as how their dynamics, combined with that of the torso, drives the movement of the entire molecule. This coupling mechanism, as we show below, differs between different molecular structures.

Since all legs are alkyl chains, with different branching configurations, connected to the torso

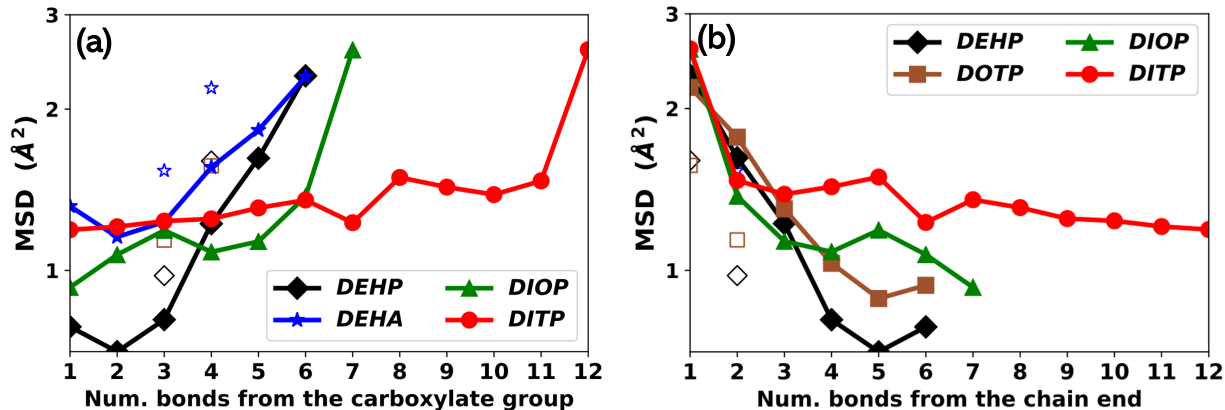


Figure 12: MSD values, measured at 20 ps, of C atoms in the legs of selected plasticizers as functions of (a) distance from the carboxylate group and (b) distance from the free chain end. Both distances are measured in terms of the number of covalent bonds. Solid markers linked by solid lines are C atoms on the main chain of the leg, while empty markers are those on the side branch.

via a carboxylate ester group, their dynamics share common features. Figure 12 shows the MSD of individual C atoms on the leg measured at the $t = 20$ ps mark, which for most plasticizers is near the end of the quasi-plateau (fig. 11) and captures the local fluctuation. As shown in fig. 12(a), the dynamics of each C atom depends on their distance from the ester group. Carbon atoms in close proximity to the ester group are slower in their movement, which is expected because the polar ester group (1) may be immobilized due to binding with other polar groups (from either PVC or the plasticizer) and (2) is directly connected to a less mobile torso group. For DIOP and DITP, the dynamics increases nearly monotonically with distance from the ester group. For DEHP, DOTP, and DEHA, all of which has an ethyl side branch, the second C atom is slower as it is the conjunction point between the main and side branches. Atoms on the side branch are consistently faster than those on the main branch, which can be attributed to its shorter length. The same MSD data are replotted in fig. 12(b) against the distance from the free leg end. Strikingly, mobility of the main-branch free-end C atom is nearly the same for different plasticizers. The dynamics slows down as we move away from the end. The second atom on DIOP and DITP is slightly slower because it, again, is a branching point, but overall the dynamics near the free end is more homogeneous between different plasticizers and less dependent on the

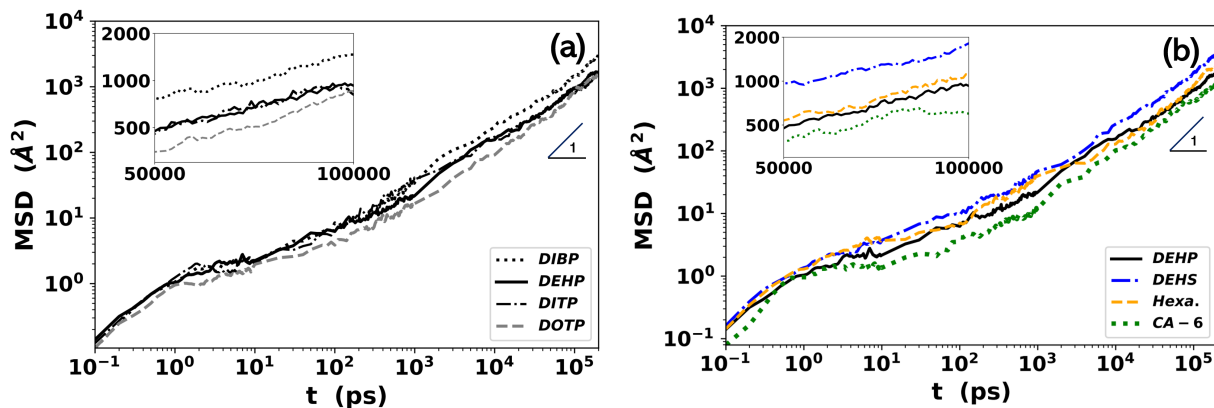


Figure 13: MSD of C atoms on the torso of plasticizers at 400K: (a) ortho-Phthalates and terephthalates; (b) non-phthalates (DEHP included as a reference).

specific plasticizer type (than the dynamics near the ester-group end in fig. 12(a)). For the side branch, dynamics of the free-end atom is slower than that of the main branch because of its shorter length, which for DEHP, DEHA, and DOTP contains only two C atoms. Constraints of the other end, i.e., the branching point and ester group, is thus more directly felt. This effect is smaller in the main branch because plasticizers shown in fig. 12 have at least 6 C atoms on the main branch. Overall, we may conclude that the dynamics of individual atoms on the leg is influenced by their distance to (1) the carboxylate ester group, (2) nearest branching point, and (3) free end. MSD shown in fig. 11 is for the averaged position (COM) of all different leg C atoms.

We now examine how different MDPs affect leg dynamics as well as the dynamics of the whole molecule.

(I) Leg size

Comparing ortho-phthalates with similar branching configuration, leg fluctuation dynamics becomes faster with increasing leg length, i.e., DITP (13) > DIOP (8) > DIBP (4) (see fig. 11(a)). This can be explained following the same argument as in section 3.2.1 and section 3.2.2: i.e., a longer alkyl chain contains more non-polar aliphatic C atoms with no specific interaction with PVC, which have higher freedom for fluctuation. Stronger fluctuation in the leg loosens the binding between the ester group and nearby PVC segments. Indeed, as shown in fig. 12(a), even the C atom closest to the ester group fluctuates

faster with increasing leg length (compare DIOP and DITP). Although longer chains also have higher total friction, which would reduce mobility, at the lower temperature of 300K, the thermodynamic factor of polar-polar interaction seems to have dominated. At higher temperatures, dynamical factors such as friction become more important. As shown in fig. 13(a), at 400K, the order becomes reversed: DITP has lower mobility than DIBP. This explains the conflicting experimental observations on the leg size effect as discussed in section 3.1.3. Our 300K case shows typical low-temperature thermodynamics-dominated behavior, where mobility increases with leg length, whereas our 400K case is in the high-temperature kinetics-dominated regime where mobility decreases with leg length.

(II) Leg branching configuration

Same as the torso case (fig. 5(a)), the leg dynamics of DEHP is also significantly suppressed compared with DIOP (8) (fig. 11(a)), which has the same C number in the legs. In fig. 12(a), for DEHP, C atoms near the ester group is most severely suppressed in comparison with DIOP (8). This also shows that the dynamics of the ester group itself must also have reduced, which can then bind more firmly with nearby PVC polar sites and increase its compatibility (section 3.2.1). Existence of a branching point near the ester group helps to fasten the chain and suppress its fluctuation. In polymer dynamics, it is well known that the relaxation of branched chains is much slower than that of linear chains, as the movement of the branching point would require simultaneous and cooperative relaxation of all branches⁹³. In the DEHP example, the branching point connects with an ethyl group and an n-butyl group, both would have to move in the same direction for the branching point to move.

(III) Substitution positions

Comparing DEHP (8) and DOTP (8), the leg configuration is identical. As a result, leg dynamics is very similar between the two cases (fig. 11(b)) while DOTP has clearly slower torso dynamics (fig. 5(b)). Therefore, unlike the previous MDPs, the effect of substitution position does not directly affect leg dynamics. Similar to the argument we made above

about branched legs, here we also attempt to explain this observation from the cooperative movement of the two legs. In DOTP, the two legs are in a para-position, i.e., substituted at opposite sides of the benzene ring, and torso movement is determined by the tug of war between the legs. The legs will have to coordinate in the same direction for the torso to move. By contrast, for ortho-substitution (DEHP), the legs extend in the same direction and their movements, even not well synchronized, do not restrict the torso movement (somewhat like the flutter kick in swimming). This effect is dynamical in nature and DOTP is slower than DEHP at both 300K (fig. 5(b)) and 400K (fig. 13(b)).

(IV) Number of legs

Adding a third leg, e.g., in TOTM (8), further slows down the dynamics compared with both DEHP (8) and DOTP (8) for the same reason: torso movement now requires the cooperative motion between all three legs. It is clear that the leg dynamics itself is again unaffected (compared with DEHP and DOTP in fig. 11(b)) except at the long time limit ($\mathcal{O}(100)$ ns), where leg relaxation is likely dragged down by the slower torso movement.

(V) Torso structure

Comparing DEHA (8) and DEHP (8) in fig. 12, which have identical leg configuration, we note that the MSD of the free end of their legs is nearly the same. However, for mobility of the other (ester) end, DEHA is much higher than DEHP. This indicates that the ester group itself has much higher mobility when the benzene ring in the torso is replaced by an aliphatic chain. The effect is not surprising considering that a linear carbon chain is leaner in shape, much more flexible, and also less polar than a benzene ring, all of which contribute to higher torso mobility, which then enhances leg mobility. This view can be confirmed by the accelerated dynamics of the torso of DEHA and DEHS, starting from very short ($\mathcal{O}(0.1)$ ps) time scales, compared with the DEHP case (fig. 5(c)). Leg dynamics is also faster (fig. 11(c)), but significant deviation from the DEHP curve is found slightly later at the $\mathcal{O}(1)$ ps time scale, which is thus a consequence of faster torso fluctuations. Replacing

benzene with cyclohexane (Hexamoll (9)) can similarly speed up the torso dynamics, but to a much lesser degree than linear torso structures, which is attributed to the bulkier shape and less conformational freedom of the ring structure. As such, although the mobility of Hexamoll, in terms of both the torso (fig. 5(c)) and leg MSD (fig. 11(c)), is higher than DEHP, it is not noticeably higher than DINP (9). Finally, for changing torso structure, although thermodynamic factors, such as the higher polarity of the benzene group, are relevant, enhanced mobility of aliphatic torso groups is mostly attributed to kinetic factors such as steric effects and conformational flexibility. Therefore, the effect does not change with temperature – aliphatic dicarboxylates remain more mobile than DEHP at the higher temperature of 400K (fig. 13(b)).

(VI) Torso size

Between the only pair (DEHA (8) and DEHS (8)) where this MDP can be investigated, its effect is only noticeable in an intermediate time range of $\mathcal{O}(10^2)$ to $\mathcal{O}(10^4)$ ps, beyond which the MSD curves of both the torso (fig. 5(c)) and the legs (fig. 11(c)) are statistically indistinguishable. Within the intermediate time scales, DEHS is slower than DEHA, which is expected for its larger size (longer backbone), but the effect does not seem to significantly affect the long-term diffusion behavior, perhaps because the torso size is not substantially apart between the two plasticizers.

(VII) Citrate structure

Comparison between citrates and traditional ortho-phthalates is more complex for the large number of molecular features that have changed at the same time. Citrates have three legs and four polar ester groups connected to a single quaternary C atom. Their lower compatibility, indicating overall weaker binding with PVC, would predict higher mobility. However, the additional leg as well as the lack of conformational degree of freedom in the quaternary C atom are both detrimental to molecular mobility. Their torso movement, as we have seen in fig. 5(e), is suppressed (compared with DEHP) across most of the temporal

spectrum, while their leg mobility (fig. 11(e)), is actually faster than DEHP in the quasi-plateau and early subdiffusive time ranges ($\mathcal{O}(1)$ ps to $\mathcal{O}(10)$ ns). Faster leg movement of citrates can be attributed to several factors including the weakened binding of their ester groups with PVC, their shorter legs, and linear leg configuration (as discussed above, branching in the legs of DEHP slows down its relaxation). Nevertheless, leg dynamics of citrates is exceeded by DEHP at longer time ($\mathcal{O}(100)$ ns) as it is eventually hindered by the slow torso motion. Kinetic factors are still more important than thermodynamics (i.e., weakened binding with PVC). For this reason, at the elevated temperature of 400K (fig. 13(b)), CA-6 mobility is still lower than that of DEHP (same as 300K).

Overall, with the exception of leg size, where the competition between thermodynamic and kinetic factors gives rise to opposite trends in molecular mobility at different temperatures, effects of other MDPs are dominated by kinetic factors such as the complex relaxation dynamics of plasticizer molecules. Theoretical understanding of the relaxation mechanisms of penetrant molecules of complex chemical structures and interactions in a polymer matrix is necessary for the prediction of plasticizer migration behaviors.

4 Conclusions

Using our recently reported molecular modeling and simulation protocol, we perform a comprehensive study on the performance of a wide variety of plasticizers on PVC materials, including linear-legged ortho-phthalates, branched-legged ortho-phthalates, terephthalates, trimellitates, aliphatic dicarboxylates, and citrates (see table 1). Plasticizer performance is predicted from molecular simulation based on three metrics – compatibility between the plasticizer and PVC, plasticization efficiency, and plasticizer mobility. Variations in chemical structure between these plasticizers are classified into seven molecular design parameters and effects of each MDP on all three performance metrics are analyzed and discussed. Previous experimental studies on plasticizer performance are also reviewed and analyzed in the same framework of these seven MDPs.

Our simulation results generally agree with available experimental data with few exceptions. Our observations show that optimization of plasticizer performance requires trade off between demands in different performance metrics. Specific effects of each MDP are summarized in section 3.1.4, which provides guidelines for plasticizer molecular design.

Attempts are then made to discuss the molecular mechanisms behind the observed relationships between molecular structure and plasticizer performance. For thermodynamic compatibility, our analysis shows that a simple argument based on the extent of polar-polar interactions between the plasticizer and the host PVC can only explain some of the MDP effects, whereas in many cases, complex molecular conformation changes during mixing and the resulting steric repulsion effects are also important. Likewise for plasticization efficiency, a simple argument based on intermolecular binding affinity would make the wrong prediction in most cases, whereas dynamical factors including molecular mobility and flexibility are often more important. For comparison at the same mass fraction, molecular weight, which determines the plasticizer number density, is also an important consideration. For plasticizer mobility, the most interesting finding is that with increasing alkyl side chain length (leg size), the mobility increases at lower temperature (300 K) but decreases at higher temperature (400 K). This is attributed to the different relative importance between thermodynamic and kinetic factors at different temperature levels. The finding well explains the seemingly conflicting experimental observations on the effects of this MDP in the literature. For other MDPs, plasticizer mobility is dominated by kinetic factors. Although a complete theory is currently out of reach, intuitive arguments can be made considering the detailed relaxation dynamics of complex plasticizer molecules. Through our discussion, it is also clear that different performance metrics are intricately coupled with non-trivial mutual effects.

Finally, on the general mechanism of plasticization, we observe that PVC segmental dynamics is not substantially affected at small to intermediate time scales where local fluctuations and caging effects are important. Introducing plasticizers only seems to accelerate the dynamics at larger scales where cooperative motions between molecules become important.

Acknowledgment

The authors acknowledge the financial support by the Natural Sciences and Engineering Research Council (NSERC) of Canada (RGPIN-2014-04903, CRDPJ-514051-17) and Canadian General Tower, Ltd. We also acknowledge Compute/Calcul Canada for its allocation of computing resource. DL would like to thank the China Scholarship Council (CSC) for supporting his doctoral study at McMaster University (No. 201500090106). This work is also made possible by the facilities of the Shared Hierarchical Academic Research Computing Network (SHARCNET: www.sharcnet.ca).

A Chemical structures and names of additional plasticizers

Various plasticizers investigated in previous experimental studies have been referenced in our discussion. Some of them are not covered by our MD simulations. For the reader's convenience, detailed chemical structures of representative additional plasticizers are listed in table 5. Plasticizers covered by our MD simulations (thus already included in table 1) but also widely studied in experiments, including DEHP (sometimes also referred to as DOP), DEHA (sometimes also referred to as DOA), DEHS (sometimes also referred to as DOS), CA-4 (also referred to as ATBC), and CA-6 (also referred to as ATHC) are already shown in table 1 and thus not repeated here.

For plasticizers of the same family with only varying N_C (indicated by the number between parenthesis following each name), only one representative structure is shown in the tables and the rest can be inferred by their names.

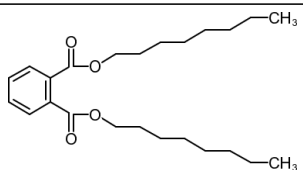
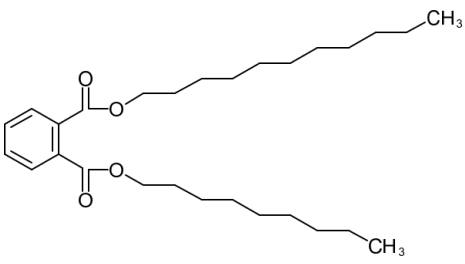
- For DBP (4) or dibutyl phthalate, DPP (5) or dipentyl phthalate, DHP (6) or dihexyl phthalate, DHepP (7) or diheptyl phthalate (using Hep for heptyl here because H stands for hexyl in this study), DNP (9) or dinonyl phthalate, DDP (10) or didecyl phthalate, and DTDP (13) or ditridecyl phthalate, which all have linear alkyl chains as legs, the reader is referred to the structure of DnOP (8).
- For DIHepP (7) or diisoheptyl phthalate, DIDP (10) or diisodecyl phthalate, and DIUP (11)

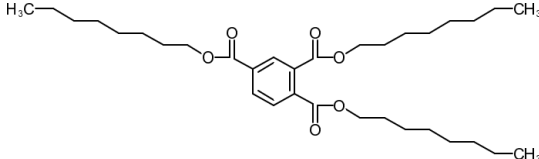
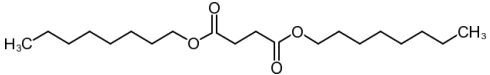
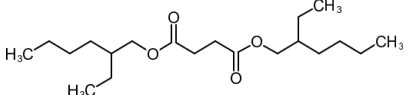
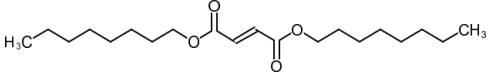
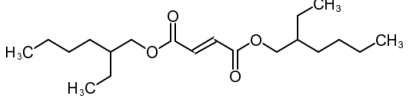
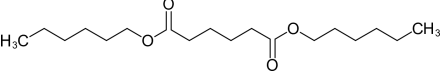
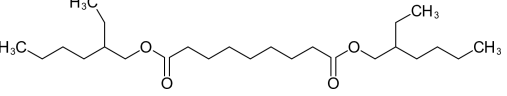
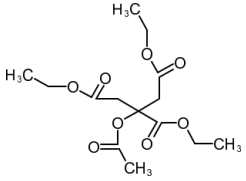
or diisoundecyl phthalate, all of which have isoalkyl legs with the methyl group attached to the penultimate C atom on the main branch, the reader is referred to the structure of DIOP (8) shown in table 1.

- For DESu (2) or diethyl succinate, DBSu (4) or dibutyl succinate, and DHSu (6) or dihexyl succinate, which are succinates with linear alkyl legs, the reader is referred to the structure of DnOSu (8).
- For DEM (2) or diethyl maleate, DBM (4) or dibutyl maleate, and DHM (6) or dihexyl maleate, which are maleates with linear alkyl legs, the reader is referred to the structure of DnOM (8).
- For DIOA (8), which is an adipate with isooctyl legs, the reader is referred to DINA (9) in table 1.

Note that we explicitly specify the “n” in DnOx (8) – x may be P for phthalate, A for adipate, S for sebacate, Su for succinate (to be distinguished from sebacate), or M for maleate – because DOx is sometimes used as an alias for DEHx (8) in the industry.

Table 5: Chemical structures of representative additional plasticizer molecules experimentally investigated in the literature and referenced in this study (N_C : Number of C atoms in each alkyl side chain).

Common Name	Full name	N_C	Category	Chemical Structure
DnOP	Dioctyl phthalate	8	ortho-phthalate	
911P	Nonyl undecyl phthalate	9, 11	ortho-phthalate	

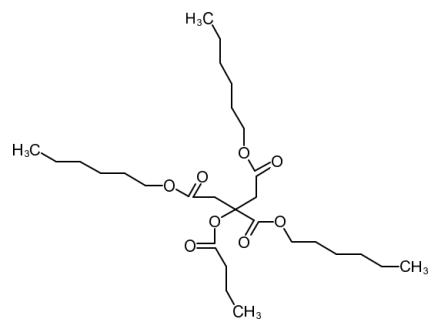
TOM	Trioctyl trimellitate	8	trimellitate	
DnOSu	Di-n-octyl succinate	8	aliphatic dicarboxylate (succinate)	
DEHSu	Bis(2-ethylhexyl) succinate	8	aliphatic dicarboxylate (succinate)	
DnOM	Di-n-octyl maleate	8	aliphatic dicarboxylate (maleate)	
DEHM	Bis(2-ethylhexyl) maleate	8	aliphatic dicarboxylate (maleate)	
DHA	Dihexyl adipate	6	aliphatic dicarboxylate (adipate)	
DEHAz	Bis(2-ethylhexyl) azelate	8	aliphatic dicarboxylate (azelate)	
Citroflex® A-2 (CA-2)	Acetyl triethyl citrate	2	citrate	

Citroflex® B-6
(CB-6)

Butyryl
trihexyl
citrate

6

citrate



References

- (1) George Matthews and George Matthews. *PVC: production, properties and uses*, volume 587. Institute of Materials London, 1996.
- (2) Mustafizur Rahman and Christopher S Brazel. The plasticizer market: an assessment of traditional plasticizers and research trends to meet new challenges. *Progress in polymer science*, 29(12):1223–1248, 2004.
- (3) John Murphy. *Additives for plastics handbook*. Elsevier, 2001.
- (4) Imran Nazir Unar, Suhail Ahmed Soomro, and Shaheen Aziz. Effect of various additives on the physical properties of polyvinylchloride resin. *Pakistan Journal of Analytical & Environmental Chemistry*, 11(2):7, 2010.
- (5) Jesse Edenbaum. *Plastics additives and modifiers handbook*. Van Nostrand Reinhold Company, 1992.
- (6) AP Tüzüm Demir and S Ulutan. Migration of phthalate and non-phthalate plasticizers out of plasticized pvc films into air. *Journal of applied polymer science*, 128(3):1948–1961, 2013.
- (7) Hanno C Erythropel, Sarah Shipley, Aurélie Börmann, Jim A Nicell, Milan Maric, and Richard L Leask. Designing green plasticizers: Influence of molecule geometry and alkyl chain length on the plasticizing effectiveness of diester plasticizers in pvc blends. *Polymer*, 89:18–27, 2016.
- (8) Federica Chiellini, Marcella Ferri, Andrea Morelli, Lucia Dipaola, and Giuseppe Latini. Perspectives on alternatives to phthalate plasticized poly (vinyl chloride) in medical devices applications. *Progress in Polymer Science*, 38(7):1067–1088, 2013.
- (9) L Bernard, B Décaudin, M Lecoœur, D Richard, D Bourdeaux, R Cueff, V Sautou, Armed Study Group, et al. Analytical methods for the determination of dehp plasticizer alternatives present in medical devices: a review. *Talanta*, 129:39–54, 2014.

- (10) Sailas Benjamin, Eiji Masai, Naofumi Kamimura, Kenji Takahashi, Robin C Anderson, and Panichikkal Abdul Faisal. Phthalates impact human health: epidemiological evidences and plausible mechanism of action. *Journal of hazardous materials*, 340:360–383, 2017.
- (11) A Marcilla, Silvia García, and JC Garcia-Quesada. Migrability of pvc plasticizers. *Polymer Testing*, 27(2):221–233, 2008.
- (12) Annika Lindström and Minna Hakkarainen. Environmentally friendly plasticizers for poly (vinyl chloride)—improved mechanical properties and compatibility by using branched poly (butylene adipate) as a polymeric plasticizer. *Journal of applied polymer science*, 100(3):2180–2188, 2006.
- (13) N González and MJ Fernández-Berridi. Application of fourier transform infrared spectroscopy in the study of interactions between pvc and plasticizers: Pvc/plasticizer compatibility versus chemical structure of plasticizer. *Journal of applied polymer science*, 101(3): 1731–1737, 2006.
- (14) PR Graham. Phthalate ester plasticizers—why and how they are used. *Environmental health perspectives*, 3:3–12, 1973.
- (15) LG Krauskopf. Plasticizer structure/performance relationships. *Journal of Vinyl Technology*, 15(3):140–147, 1993.
- (16) Leonard G Krauskopf. How about alternatives to phthalate plasticizers? *Journal of vinyl and additive technology*, 9(4):159–171, 2003.
- (17) Badra Bouchareb and Mohamed Tahar Benaniba. Effects of epoxidized sunflower oil on the mechanical and dynamical analysis of the plasticized poly (vinyl chloride). *Journal of applied polymer science*, 107(6):3442–3450, 2008.
- (18) Puyou Jia, Lihong Hu, Guodong Feng, Caiying Bo, Meng Zhang, and Yonghong Zhou. Pvc

- materials without migration obtained by chemical modification of azide-functionalized pvc and triethyl citrate plasticizer. *Materials Chemistry and Physics*, 190:25–30, 2017.
- (19) Hanno C Erythropel, Milan Maric, and David G Cooper. Designing green plasticizers: influence of molecular geometry on biodegradation and plasticization properties. *Chemosphere*, 86(8):759–766, 2012.
- (20) Hanno C Erythropel, Patrick Dodd, Richard L Leask, Milan Maric, and David G Cooper. Designing green plasticizers: Influence of alkyl chain length on biodegradation and plasticization properties of succinate based plasticizers. *Chemosphere*, 91(3):358–365, 2013.
- (21) Hanno C Erythropel, Tobin Brown, Milan Maric, Jim A Nicell, David G Cooper, and Richard L Leask. Designing greener plasticizers: Effects of alkyl chain length and branching on the biodegradation of maleate based plasticizers. *Chemosphere*, 134:106–112, 2015.
- (22) PH Foss and MT Shaw. Thermodynamics of pvc–plasticizer interaction: A review. *Journal of Vinyl Technology*, 7(4):160–171, 1985.
- (23) Hwee-Khim Boo and Montgomery T Shaw. Application of the unifac-fv group contribution method to the prediction of relative compatibility of plasticizers with pvc. *Journal of Vinyl Technology*, 10(2):77–83, 1988.
- (24) Hwee-Khim Boo and MT Shaw. Gelation and interaction in plasticizer/pvc solutions. *Journal of Vinyl Technology*, 11(4):176–179, 1989.
- (25) JT Van Oosterhout and M Gilbert. Interactions between pvc and binary or ternary blends of plasticizers. part i. pvc/plasticizer compatibility. *Polymer*, 44(26):8081–8094, 2003.
- (26) Paul J Flory. *Principles of polymer chemistry*. Cornell University Press, 1953.
- (27) CE Anagnostopoulos, AY Coran, and HR Gamrath. Polymer–diluent interactions. i. a new micromethod for determining polyvinyl chloride-diluent interactions. *Journal of applied polymer science*, 4(11):181–192, 1960.

- (28) DJ David, NA Rotstein, and TF Sincock. The application of miscibility parameter to the measurement of polymer-plasticizer compatibility. *Polymer Bulletin*, 33(6):725–732, 1994.
- (29) Leonard C Grotz. Diffusion of dioctyl phthalate into poly (vinyl chloride). *Journal of Applied Polymer Science*, 9(1):207–212, 1965.
- (30) Robson F Storey, Kenneth A Mauritz, and B Dwain Cox. Diffusion of various dialkyl phthalate plasticizers in pvc. *Macromolecules*, 22(1):289–294, 1989.
- (31) Kenneth A Mauritz, Robson F Storey, and Scott E George. A general free volume-based theory for the diffusion of large molecules in amorphous polymers above the glass temperature. i. application to di-n-alkyl phthalates in pvc. *Macromolecules*, 23(2):441–450, 1990.
- (32) Christopher S Coughlin, Kenneth A Mauritz, and Robson F Storey. A general free-volume-based theory for the diffusion of large molecules in amorphous polymers above glass temperature. 5. application to dialkyl adipate plasticizers in poly (vinyl chloride). *Macromolecules*, 24(8):2113–2116, 1991.
- (33) L Ramos-de Valle and M Gilbert. Pvc/plasticizer compatibility. 3. dynamic mechanical and tensile properties. *Plastics Rubber and Composites Processing and Applications*, 15(4):207–212, 1991.
- (34) Yanjun Wang, Changlin Zhou, Yao Xiao, Shiyi Zhou, Chune Wang, Xiaofeng Chen, Kai Hu, Xiaowei Fu, and Jingxin Lei. Preparation and evaluation of acetylated mixture of citrate ester plasticizers for poly (vinyl chloride). *Iranian Polymer Journal*, 27(6):423–432, 2018.
- (35) Leonard G Krauskopf. Prediction of plasticizer solvency using hansen solubility parameters. *Journal of vinyl and additive technology*, 5(2):101–106, 1999.
- (36) Leonard I Nass and C Heiberger. Encyclopedia of pvc. vol. 1: Resin manufacture and properties. *Marcel Dekker, Inc, 270 Madison Ave, New York, New York 10016, USA, 1986. 702*, 1986.
- (37) George Wypych. *Handbook of plasticizers*. ChemTec Publishing, 2004.

- (38) Charles E Wilkes, James W Summers, Charles Anthony Daniels, and Mark T Berard. *PVC handbook*, volume 184. Hanser Munich, 2005.
- (39) LI Nass and CA Heiberger. *Encyclopedia of PVC, 2nd Ed.* Marcel Dekker, New York, 1988.
- (40) FW Clark. Plasticizer. *Chem. Ind*, 60:225–230, 1941.
- (41) William Aiken, Turner Alfrey Jr, Arthur Janssen, and Hermann Mark. Creep behavior of plasticized vinylite vynw. *Journal of Polymer Science*, 2(2):178–198, 1947.
- (42) A Marcilla and M Beltran. Mechanisms of plasticizers action. *Handbook of plasticizers*, pages 107–120, 2004.
- (43) Karl G Wagner, Martin Maus, Andreas Kornherr, and Gerhard Zifferer. Glass transition temperature of a cationic polymethacrylate dependent on the plasticizer content–simulation vs. experiment. *Chemical physics letters*, 406(1-3):90–94, 2005.
- (44) Hakima Abou-Rachid, Louis-Simon Lussier, Sophie Ringuette, Xavier Lafleur-Lambert, Mounir Jaidann, and Josée Brisson. On the correlation between miscibility and solubility properties of energetic plasticizers/polymer blends: modeling and simulation studies. *Propellants, Explosives, Pyrotechnics*, 33(4):301–310, 2008.
- (45) Yu Zhao, Xiaohong Zhang, Wei Zhang, Hongjun Xu, Wuxi Xie, Jiaojiao Du, and Yingzhe Liu. Simulation and experimental on the solvation interaction between the gap matrix and insensitive energetic plasticizers in solid propellants. *The Journal of Physical Chemistry A*, 120(5):765–770, 2016.
- (46) Yuxing Zhou and Scott T Milner. Average and local T_g shifts of plasticized pvc from simulations. *Macromolecules*, 51(10):3865–3873, 2018.
- (47) Dongyang Li, Kushal Panchal, Roozbeh Mafi, and Li Xi. An atomistic evaluation of the compatibility and plasticization efficacy of phthalates in poly (vinyl chloride). *Macromolecules*, 51(18):6997–7012, 2018.

- (48) Robert J Ouellette and J David Rawn. *Organic chemistry: structure, mechanism, and synthesis*. Elsevier, 2014.
- (49) J. R. Maple, M. J. Hwang, T. P. Stockfisch, U. Dinur, M. Waldman, C. S. Ewig, and A. T. Hagler. Derivation of class-II force-fields .1. Methodology and quantum force-field for the alkyl functional-group and alkane molecules. *J. Comput. Chem.*, 15:162–182, 1994.
- (50) MJ Hwang, TP Stockfisch, and AT Hagler. Derivation of class ii force fields. 2. derivation and characterization of a class ii force field, cff93, for the alkyl functional group and alkane molecules. *Journal of the American Chemical Society*, 116(6):2515–2525, 1994.
- (51) Sergei Shenogin and Rahmi Ozisik. Xenoview. <http://xenoview.mat.rpi.edu>, 2010.
- (52) Leandro Martínez, Ricardo Andrade, Ernesto G Birgin, and José Mario Martínez. Packmol: a package for building initial configurations for molecular dynamics simulations. *Journal of computational chemistry*, 30(13):2157–2164, 2009.
- (53) Steve Plimpton, Paul Crozier, and Aidan Thompson. Lammmps-large-scale atomic/molecular massively parallel simulator. *Sandia National Laboratories*, 18:43–43, 2007.
- (54) Huai Sun. Compass: an ab initio force-field optimized for condensed-phase applications overview with details on alkane and benzene compounds. *The Journal of Physical Chemistry B*, 102(38):7338–7364, 1998.
- (55) M. P. Allen and D. J. Tildesley. *Computer Simulation of Liquids*. Oxford University Press, New York, 1989.
- (56) D. Frenkel and B. Smit. *Understanding Molecular Simulation: from Algorithms to Applications*. Academic Press, London, 2nd edition, 2002.
- (57) P. P. Ewald. The calculation of optical and electrostatic grid potential. *Annalen Der Physik*, 64:253–287, 1921.

- (58) W. Shinoda, M. Shiga, and M. Mikami. Rapid estimation of elastic constants by molecular dynamics simulation under constant stress. *Phys. Rev. B*, 69:134103, 2004. doi: 10.1103/PhysRevB.69.134103.
- (59) P. A. Small. Some factors affecting the solubility of polymers. *J. Appl. Chem*, 3:71–80, 1953. doi: 10.1002/jctb.5010030205.
- (60) David F Cadogan and Christopher J Howick. Plasticizers. *Kirk-Othmer Encyclopedia of Chemical Technology*, 2000.
- (61) Luis Ramos-de Valle and Marianne Gilbert. Pvc/plasticizer compatibility: evaluation and its relation to processing. *Journal of Vinyl Technology*, 12(4):222–225, 1990.
- (62) A Marcilla and JC Garcia. Rheological study of pvc plastisols during gelation and fusion. *European polymer journal*, 33(3):349–355, 1997.
- (63) W Riemenschneider. Hm bolt in ullmann’s encyclopedia of industrial chemistry, vol. 13, 2005.
- (64) Anna Wypych. *Databook of plasticizers*. Elsevier, 2017.
- (65) Robert C Weast, Melvin J Astle, William H Beyer, et al. *CRC handbook of chemistry and physics*, volume 69. CRC press Boca Raton, FL, 1988.
- (66) Robert A Lewis. *Hawley’s condensed chemical dictionary*. John Wiley & Sons, 2016.
- (67) MV Titow. *PVC technology*. Springer Science & Business Media, 2012.
- (68) Allan F. M. Barton. Solubility parameters. *Chem. Rev.*, 75:731–753, 1975. doi: 10.1021/cr60298a003.
- (69) Phillip Choi. A re-examination of the concept of ildebrand solubility parameter for polymers. *Macromol. Rapid Commun*, 23:484–487, 2002. doi: 10.1002/1521-3927(20020501)23:8<484::AID-MARC484>3.0.CO;2-K.

- (70) M. Rubinstein and R. H. Colby. *Polymer Physics*. Oxford University Press, New York, 2003.
- (71) Paul H Daniels and Adam Cabrera. Plasticizer compatibility testing: Dynamic mechanical analysis and glass transition temperatures. *Journal of Vinyl and Additive Technology*, 21(1): 7–11, 2015.
- (72) Jie Chen, Zengshe Liu, Ke Li, Jinrui Huang, Xiaolan Nie, and Yonghong Zhou. Synthesis and application of a natural plasticizer based on cardanol for poly (vinyl chloride). *Journal of Applied Polymer Science*, 132(35), 2015.
- (73) Kushal Panchal. The effects of molecular structure and design on the plasticizer performance through coarse-grained molecular simulation. Master's thesis, McMaster University, 2018.
- (74) GS Park and Tran Van Hoang. Diffusion of additives and plasticizers in poly(vinyl chloride)—i. the 1:2 double disc method for obtaining the diffusion coefficient of additives in polymers. *European Polymer Journal*, 15:817–822, 1979.
- (75) GS Park and M Saleem. Diffusion of additives and plasticizers in poly (vinyl chloride)—v. diffusion of n-hexadecane and ddt in various poly (vinyl chloride)/dialkylphthalate compositions. *Journal of membrane science*, 18:177–185, 1984.
- (76) PJF Griffiths, KG Krikor, and GS Park. Diffusion of additives and plasticizers in poly(vinyl chloride): 4. a programmed temperature technique for the determination of the diffusion parameters of three dialkylphthalates. *European Polymer Journal*, 16:779–783, 1980.
- (77) PJF Griffiths, K G Krikor, and GS Park. *Diffusion of Additives and Plasticizers in Poly(Vinyl Chloride)-III Diffusion of Three Phthalate Plasticizers in Poly(Vinyl Chloride)*, pages 249–260. Springer, 1984.
- (78) Christopher S Coughlin, Kenneth A Mauritz, and Robson F Storey. A general free volume based theory for the diffusion of large molecules in amorphous polymers above T_g . 3. theoretical conformational analysis of molecular shape. *Macromolecules*, 23(12):3187–3192, 1990.

- (79) Christopher S Coughlin, Kenneth A Mauritz, and Robson F Storey. A general free volume based theory for the diffusion of large molecules in amorphous polymers above T_g . 4. polymer-penetrant interactions. *Macromolecules*, 24(7):1526–1534, 1991.
- (80) Bin Sun, Bharat Indu Chaudhary, Chun-Yin Shen, Di Mao, Dong-Ming Yuan, Gan-Ce Dai, Bin Li, and Jeffrey M Cogen. Thermal stability of epoxidized soybean oil and its absorption and migration in poly (vinylchloride). *Polymer Engineering & Science*, 53(8):1645–1656, 2013.
- (81) Guodong Feng, Lihong Hu, Yan Ma, Puyou Jia, Yun Hu, Meng Zhang, Chengguo Liu, and Yonghong Zhou. An efficient bio-based plasticizer for poly (vinyl chloride) from waste cooking oil and citric acid: synthesis and evaluation in pvc films. *Journal of Cleaner Production*, 189:334–343, 2018.
- (82) M. C. Reed, H. F. Klemm, and E. F. Schulz. Removal by Oil, Soapy Water, and Dry Powders. *Industrial & Engineering Chemistry*, 46(6):1344–1349, 1954. doi: 10.1021/ie50534a060.
- (83) A Marcilla, S Garcia, and JC Garcia-Quesada. Study of the migration of pvc plasticizers. *Journal of Analytical and Applied Pyrolysis*, 71(2):457–463, 2004.
- (84) Joshua Kastner, David G. Cooper, Milan Marić, Patrick Dodd, and Viviane Yargeau. Aqueous leaching of di-2-ethylhexyl phthalate and “green” plasticizers from poly(vinyl chloride). *Sci. Total Environ.*, 432:357–364, 2012. doi: 10.1016/j.scitotenv.2012.06.014.
- (85) Nils H. Nilsson, Jeanette Schjøth Eskesen, Bjørn Malmgren-Hansen, and Eva Jacobsen. Determination of Migration Rates for Certain Phthalates. Technical Report 149, The Danish Environmental Protection Agency, Copenhagen, 2016.
- (86) W Paul, D Bedrov, and GD Smith. Glass transition in 1, 4-polybutadiene: Mode-coupling theory analysis of molecular dynamics simulations using a chemically realistic model. *Physical Review E*, 74(2):021501, 2006.

- (87) D Fragiadakis and CM Roland. Role of structure in the α and β dynamics of a simple glass-forming liquid. *Physical Review E*, 95(2):022607, 2017.
- (88) Edmund H Immergut and Herman F Mark. Principles of plasticization. In Norbert A Platzler, editor, *Plasticization and Plasticizer Processes*, volume 48 of *Advances in Chemistry*, chapter 1, pages 1–26. ACS Publications, 1965.
- (89) Von F Würstlin and H Klein. O-phthalsäuredialkylester als pvc-weichmacher. *Die Makromolekulare Chemie: Macromolecular Chemistry and Physics*, 16(1):1–9, 1955.
- (90) Li Xi, Manas Shah, and Bernhardt L Trout. Hopping of water in a glassy polymer studied via transition path sampling and likelihood maximization. *The Journal of Physical Chemistry B*, 117(13):3634–3647, 2013.
- (91) Masao Doi and Samuel Frederick Edwards. *The theory of polymer dynamics*, volume 73. oxford university press, 1988.
- (92) Oluseye Adeyemi, Shiping Zhu, and Li Xi. Dynamics and Stress Relaxation of Bidisperse Polymer Melts with Unentangled and Moderately Entangled Chains. *Physics of Fluids*, 33(6):063105, 2021. doi: 10.1063/5.0053790.
- (93) Ronald G Larson. Predicting the flow of real polymers. *Science*, 333(6051):1834–1835, 2011.